Doctoral Thesis at NTNU

Hagbart Skage Alsos

Analysis of ship grounding

Assessment of ship damage, fracture and hull girder behavior

Trondheim, April 2008

Norwegian University of Science and Technology
Faculty of Engineering and Technology
Department of Marine Technology

NTNU
Innovation and Creativity

NTNU

Norwegian University of Science and Technology

Doctoral thesis
for the degree of Doctoral Engineer

Faculty of Engineering and Technology
Department of Marine Technology

ISBN N/A (printed version)
ISBN N/A (electronic version)
ISSN 1503-8181

Doctoral theses at NTNU, 2008:N/A

Printed by NTNU-trykk

Abstract

The present work is concerned with problems related to grounding of ships. This ranges from prediction of fracture to analysis of hull girder loads during grounding. The thesis is composed as a collection of articles and consists of two parts. The first part gives an introduction, background and summarizes the findings from the PhD. work. The second part presents the articles.

A significant part of the thesis is dedicated to the work on fracture. Reliable prediction of fracture initiation and propagation is essential in order to estimate the hull indentation resistance and the oil spill during grounding. In order to better predict the onset of fracture two relatively advanced criteria are investigated. These are the BWH instability criterion, Alsos et al. (2008b), and the RTCL damage criterion, Törnqvist (2003), respectively. These criteria are implemented into LS-DYNA by the author and verified in simulations. In addition, problems related to the mesh sensitivity close to the point of fracture is discussed. An attempt on improving the existing way of dealing with this effect is made.

The response of stiffened panels when subjected to extreme lateral loads are investigated by testing. The panels are indented beyond the point of fracture. The results from these tests are further compared with numerical simulations where fracture is predicted using the BWH and the RTCL failure criteria.

An important issue is the size and shape of the sea floor in grounding analysis. As little information is generally available, the thesis discusses sea floor shape in view of the resistance to indentation of the ship bottom. From this, characteristic scenarios are defined. The resistance to indentation is analyzed for a typical oil tanker for various positions of contact. The interaction between global hull girder bending effects and local indentation actions is also addressed.

Ships which run aground with forward speed may experience damage of over the entire hull girder length. Analysis of this is made complex by the temporal and spatial extent which this implies. Thus, complete finite element simulation becomes very demanding. A new, simplified approach to estimate the contact actions and the subsequent damage due to grounding is therefore presented. Excellent agreement is obtained between the simplified procedure and numerical simulations.

The application of the simplified sliding force method is illustrated by simplified

simulations of dynamic/powered grounding. It has been shown that the process is indeed dynamic and that large hull girder bending moments and shear forces are formed, especially during the initial impact. These shear forces and bending moments may become larger than the minimum still water rule requirements set by the classification society. This corelates well with observations made by Pedersen (1994) and Simonsen (1997a).

Acknowledgments

This work has been carried out under the supervision of Professor Jørgen Amdahl at the Department of Marine Technology at the Norwegian University of Science and Technology. I am most grateful for the guidance, support and the enthusiasm he has shown during the past three and a half years.

I also wish to thank Professor Odd Sture Hopperstad for his advices and fruitful discussions in the work on fracture and instability mechanics. His involvement in the project has been essential for the development of the BWH criterion.

Laboratory testing constituted an important part of the work. Testing took part in the NTNU laboratory facilities at Tyholt with good assistance from Roar Schjetne and Eirk Fleischer.

I would like to warmly thank all my friends and colleagues at the department for their support and for making these years enjoyable. Although it was hard work, we still managed to have a good time!

I also wish to thank friends and colleagues I met at various conferences and workshops. Among them I would like to mention are: Kristjan Tabri and Sören Ehlers at HUT in Finland, Florian Biehl at Germanischer Lloyds, Joep Broekhuijsen at Royal Schelde, Frank Klæbo at Marintek and Rikard Törnqvist at Det Norske Veritas.

Last but not least, I want to express my gratitude to my family, and especially to my fiance Kristin who patiently has carried the burdens of a hard working PhD. student. Thank you for your encouragements and support.

The information embedded in the present thesis is generated as a part of the EU sponsored project: Decision Support System for Ships in Degraded Condition (DSS_DC). The author is grateful for the economic support.

Synopsis

[A1] Article I:

Alsos H. S., Hopperstad O. S., Törnqvist R., Amdahl J., Analytical and numerical analysis of sheet metal instability using a stress based criterion, *Published in:*, International Journal of Solids and Structures, v 45, pp 2042–2055, 2008

Alsos et al. (2008b): In this article the Bressan Williams Hill criterion is described (BWH). This is a stress based instability criterion which requires few input parameters. The BWH criterion is analyzed analytically and compared with experimental forming limit results. In addition, the BWH criterion is implemented to LS-DYNA and applied in simulations.

The advantage by using the BWH criterion over other criteria is the simple application. In the form it is presented, no external inputs other than the material stress-strain curve is needed. Furthermore, by avoiding analysis in the local necking region, the element size sensitivity is reduced.

[A2] Article II:

Alsos H. S., Amdahl J. , On the resistance to penetration of stiffened plates – Part I: Experiment, *Submitted to:*, International Journal of Impact Engineering

Alsos and Amdahl (2008a): A series of panel indentation tests have been conducted. This article describes the observations from these tests. Five panels with varying stiffener configurations are penetrated by a conical indenter in order to "simulate" tanker grounding on a "rock". Naturally, because ship hulls are surrounded by water and often carry hazardous cargo, focus is placed on the panel resistance to fracture.

[A3] Article III:

Alsos H. S., Amdahl J., Hopperstad O. S., On the resistance to penetration of stiffened plates – Part II: Numerical analysis, *Submitted to:* International Journal of Impact Engineering

Alsos et al. (2008a): This article presents the results of finite element simulations of the panel tests described in part 1. Two state of the art failure criteria are applied in the simulations. These are the BWH criterion, [A1] and the RTCL criterion, Törnqvist (2003). For each tests, three models are analyzed, all with different element sizes. In total this gives 30 finite element models. The paper evaluates both criteria and compares the results with the experiments.

The paper also discusses alternative options to deal with the element size sensitivity at the onset of fracture. One of these are exemplified in conjunction the BWH and the RTCL criterion with promising results.

[A4] Article IV:

Alsos H. S., Amdahl J., On the resistance of tanker bottom structures during stranding, *Published in:*, Marine Structures, V 20, pp 218–231, 2007

Alsos and Amdahl (2007a): The fourth article deals with stranding of tankers and the bottom damage caused by various grounding scenarios. The attention is on the sea floor geometry. This is connected to the resistance to indentation and eventually penetration of the ship bottom.

Integrated local/global grounding analyses are also performed. During stranding, the change in tide crates grounding actions which lift the ship out of the water. In this process large hull bending moments are formed. Combined with the damaged hull cross section and the grounding actions, this may eventually provoke collapse of the hull girder.

[A5] Article V:

Alsos H. S., Amdahl J., Sliding Resistance of Ship Bottom Structures Subjected to Grounding, *Submitted to:*, Marine Structures

Alsos and Amdahl (2008b): The final article is a follow up paper of [A4]. Now the attention has shifted from static stranding to dynamic/powered grounding. The focus is on grounding on large sea floor surfaces, e.g. shoals. The bottom damage caused by grounding on shoals is referred to as sliding damage.

A simplified approach to establish the contact forces caused by the sliding damage is presented. This is applied in a series of analyses which in turn are compared with finite element "sliding" simulations. Finally, the paper presents an application for the simplified procedure. This is implemented into a simplified rigid body dynamics code for fast simulation of ship grounding in the time domain.

Other articles

The author has also taken part in the following articles. They are, however, not included in the thesis.

Alsos H. S., Amdahl J., Static and dynamic analysis of a tanker during grounding, In: PRADS, 2007

Alsos, H. S. Hopperstad, O. S., Amdahl, J.,Prediction of rupture in collision and grounding of ships using the BWH failure criterion, In: ICCGS, 2007

Alsos H. S., Amdahl J., Analysis of bottom damage caused by ship grounding, Accepted in: OMAE, 2008

Ehlers, S., Broekhuijsen, J., Alsos, H. S., Biehl, F., Tabri, K., Simulating collision response of ship side structures; a failure criteria benchmark study. *International Shipbuilding Journal.*, In press

Tabri, K., Alsos, H. S., Broekhuijsen, J., Ehlers, S. , A benchmark study on ductile failure criteria for shell elements in multiaxial stress states, In: MARSTRUCT 2007

Contents

Part I

Introduction and Thesis Summary

Chapter 1

Introduction

Historical and recent events have made it clear that ship grounding and collision represent significant hazards. This applies with respect to loss of human lives as well as severe environmental consequences. Refer for instance the "*Exxon Valdez*" accident (1989). This incident gathered much publicity due to the discharge of more than 240,000 barrels of oil (20% of the cargo) into the Prince William Sound in Alaska, USA. The environmental effect of this was beyond anyones imagination at the time. In 1997, the "*Nakhodka*", a Russian tanker carrying 19,000 tons of heavy fuel oil broke in half during storms in the Sea of Japan, with severe environmental consequences. Similarily, in November 2002, the "*Prestige*" oil tanker split in half during a storm, and sank into the Atlantic along with 77,000 tons of fuel oil. The consequence of the accident was a vast oil spill. To this end, the ship still leaks fuel oil, which pollutes the Galicia region outside Spain.

On the Norwegian coast several accidents have occurred that have caused serious public concern. In 1992 the Panama registered bulk carrier "*Arisan*" grounded near the bird nesting cliff Runde and considerable amounts of oil were threatening the ecology system in the region. In the fall of 2000 the "*Green Ålesund* "capsized close to Haugesund and "*John R*" stranded and broke in two outside Grøtøy North of Tromsø. In both cases only favorable weather conditions prevented major oil spills. More recently, (2007) the cargo ship "*MS Server*" grounded and split in half outside Fedje, Norway, see Fig. 1.1. This resulted in discharge of oil in a ecological vulnerable area.

These events demonstrate that the risk level is not acceptable, and that public awareness of sub-standard transportation systems is increasing. The risk of massive spill or casualties constitutes a threat to sustainable development. Improvement of casualty prevention measures is therefore essential to obtain the desired level of safety at sea and protection of marine ecosystems.

(a) (b)

Figure 1.1: (a) shows the bow and cargo section of "*MS Server*" which broke in two outside Fedje, Norway, after grounding. Fig (b) shows a photo of the "*New Carissa*", which run aground at the US west coast.

1.1 Background

Ship collision and grounding events represent highly non-linear processes. Scientific analysis is made complex by unknown and highly coupled effects. This involves large contact forces, extensive structural damage and unknown hydrodynamic loads. Complete analysis is made even more demanding by the temporal and spatial extent of such accidents. In the case of grounding with forward speed, so called "powered grounding", Simonsen and Hansen (2000), the ship may sustain severe damage over large parts of the ship length. Often the real duration may go on for more than 10-20 seconds. Full finite element (FE) analyses may therefore become time-consuming, especially when considering the short time steps needed for stable explicit FE solutions. This is often in the order of 10^{-6} seconds, or less. Consequently, to simplify the problem, grounding analyses are often divided into two sub tasks; internal and external mechanics, respectively.

1.1.1 External mechanics

The external mechanics of ships subjected to grounding, deals with the ship motions and hull girder loads. In other words, the overall motions are decoupled from the structural damage. This approach has been followed by Pedersen (1994) who developed analytical procedures to determine the hull girder loads for ships run-

ning aground on inclined slopes. Similar studies have been presented by Simonsen (1997b), who numerically calculated the ship motions and hull girder loads during soft grounding. Asadi and Vaughan (1990) have also presented analyses on powered grounding of ships. This was done using a simplified FE beam code to simulate the ship motions. The contact forces and hull damage was estimated by means of a Minorsky (1959) formulation and experimental data. The rigid body motions of ships subjected to stranding have been investigated by McCormick and Hudson (2001). Similarly, Petersen (1982) has presented analyses on ship motions during collision events.

1.1.2 Internal mechanics

Analysis of the internal mechanics involves the material response and the associated energy dissipation of structures when subjected to loads or deformations. According to the ISSC (International Ship Structure Committee) reports: Paik et al. (2003) and Wang et al. (2006), there are three main approaches to analyze hull damage. These are: empirical approaches, simplified analytical approaches, and analyses using the finite element method (FEM).

A classical example on an empirical approach is presented by Minorsky (1959), better known as the Minorsky method. The Minorsky method is derived from steel deformation data extracted from actual ship collisions, and describes a linear relation between the damaged steel volume and the dissipated energy. The method is simple to use and well suited for simplified estimations of the energy dissipation in ship-ship collisions. The validity of the formulation has however been questioned, because it is derived from data which stem from ship designs prior to the 1950's. Although several attempts on improving the Minorsky method are made, e.g. by Pedersen and Zhang (2000), more modern methods are generally preferred.

An alternative to empirical methods are simplified analytical methods. These are often referred to as plastic mechanisms. In simplified analyses, structural deformations are described in terms of simplified plastic mechanisms, such as yield lines, membrane zones and tearing mechanisms. These may be combined to describe more complex deformations. Wierzbicki and Thomas (1993) have for instance derived a closed form solution for the cutting resistance of plates, while Amdahl (1983) and Wierzbicki and Abramowicz (1983) have expressed relations for the crushing resistance of girder cruciforms. Examples of such methods applied in grounding analyses are presented by Simonsen and Wierzbicki (1998), Wierzbicki et al. (1998), Pedersen and Zhang (2000) and Simonsen (1997b). The advantage of the simplified approach is reasonable accuracy achieved with little computational effort. However, in order to get meaningful results, the deformation mechanism must be known prior to the analysis. It must also have a closed form analytical solution.

The simplified computations may be assembled to form so called "super ele-

ments". These may be combined to determine the collision and grounding behavior of entire structures. This is for instance substantiated by the computer based collision and grounding code DAMAGE, see Wierzbicki (1992–1999).

With the past decades advances in computer technology, the finite element (FE) method has become a viable tool in order to assess collision and grounding scenarios. An excellent summary on the scientific work conducted with the FE method is found in the 2003 and 2006 ISSC reports, Paik et al. (2003) and Wang et al. (2006). Refer also Naar et al. (2002), Samuelides et al. (2007) and Kitamura (2002).

Although the FE method represents the most advanced approach, problems related to the prediction of fracture still need to be resolved. Presently, there is no adequate method to determine both fracture initiation and propagation in large scale shell structures. This discrepancy has been investigated extensively by Törnqvist (2003) and Simonsen and Törnqvist (2004)

The internal mechanics of ship structures may also be investigated from an experimental point of view. Woisin (1979) is considered a pioneer in this field, after performing large scale bow impact tests of nuclear powered vessels in the 1960's. Amdahl and Kavlie (1992) have investigated the stranding resistance of scaled down double bottom structures. This was done by forcing a model of the seafloor, a so called "indenter", laterally into the specimens. A similar study is also reported by Wang et al. (2000).

Several large scale grounding tests were conducted during the early 1990's. Rodd and Phillips (1994) and Rodd and Sikora (1995) present results from grounding experiments where a model of a tanker, carried on rail cars, was forced horizontally over a model of the sea floor. The tests were carried out dynamically and provoked tearing damage. In the same period, collision and grounding tests were carried out by the Association of Structural Improvement of Shipbuilding in Japan (ASIS). These are reported by Paik et al. (2003) and comprized deformation of real sized girder and stringer members. Finally, the ship side response during collision events have been investigated experimentally by Wevers and Vredeveldt (1999). These are further reported by Lehmann and Peschmann (2001) and Ehlers et al. (2008).

1.2 Objectives and problem description

The present work is carried out as a part of the EU project entitled: "Decision Support System for Ships in Degraded Condition" (DSS_DC). This is an international initiative with several contributors. The consortium consist of: BMT, UK, The Technical University of Berlin, MARTEC S.p.a., Italy, Kongsberg Maritime, Norway, LODIC, Norway, SIEMENS Marine Solutions, Germany, the worlds largest cruise vessel operator, Carnival Cruises, UK and Teekay Norway, a major owner of trading and shuttle tankers. Marintek, Norway is managing the project.

The intention behind the DSS_DC project is to establish an integrated decision support system for ships in a degraded condition. This condition may for instance be caused by accidental events such as collision, grounding or fire. The decision support system will serve as guidance for the crew on how to reduce the hull girder loads, and how to bring the ship to the closest port without further damage. In an emergency situation the crew has two last resort options; either beach the ship in sheltered waters in order to stabilize the situation, or tow the ship further offshore. In the latter case the ship may risk collapse of the hull girder, as was the case for the "Prestige". Intentional grounding of ships is, nevertheless, a drastic undertaking. Before such a decision is made, the ships behavior during different grounding scenarios must be investigated.

1.2.1 Procedure to analyze grounding

Complete analysis of ship grounding is a complex undertaking. The analysis can be divided into several sub groups. A potential design procedure for grounding is presented by Amdahl et al. (1995), see Fig. 1.2. The starting point is characterizing the ship dimensions, structural scantlings, forward speed and cargo arrangement. Refer (1a) in Fig. 1.2. In this way, the structural properties, as well as the ships still water condition is established. The sea floor conditions are of paramount importance (1b). This may vary from sharp rocks to hard shoals or soft clay/sand banks. The type of damage of the ship bottom will vary significantly with the sea floor topology.

The terminology used in description of various grounding scenarios may vary in the literature. In the present work, ship grounding considers scenarios where ships either runs aground and/or settles on the sea floor. Grounding with forward speed is referred to as "powered grounding", see Simonsen and Hansen (2000). In this case the driving energy comes from the forward motion of the ship. Grounding without forward speed is referred to as "stranding". In this case, the ship is indented vertically. The driving energy comes from gravity, ebb tide and waves.

Step two (2) describes the external mechanics of the ship. The ships rigid body motions and hull girder loads may be found from information about the hydrodynamic loads and grounding excitation forces. The hydrodynamic loads may be calculated from potential theory, see Faltinsen (1999), or from simplified assumptions about hydrodynamic added mass, damping and restoring forces. The grounding actions are found from considerations of the local deformation, e.g. by using the FE method or simplified methods.

The damage of the hull girder is determined in step three (3). This step describes the internal mechanics and is closely related to step (2) in the sense that the hull damage and subsequent contact forces are coupled with the ship motions. Hull damage due to grounding is dealt with in [A4] and [A5].

One of the main concerns in step (3) is whether the hull plating and cargo tank is

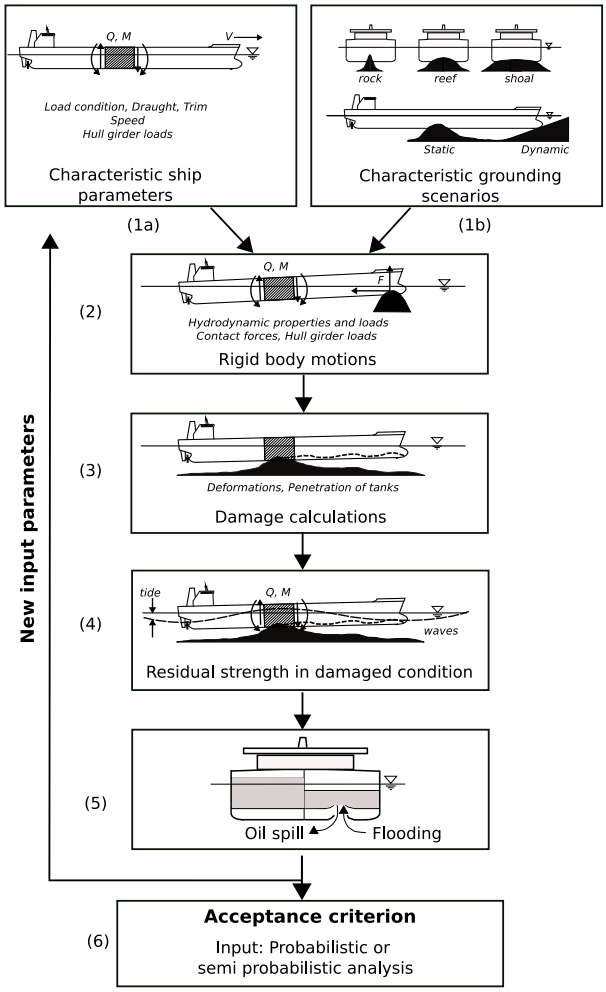

Figure 1.2: Flow chart showing the grounding analysis process.

penetrated or not. Once fracture is initiated, the hull plating may have little reserve capacity, as reported by Naar et al. (2002) and Simonsen and Lauridsen (2000). Another concern related to hull penetration is water filling and oil spill. Focus on ductile fracture is addressed in [A1], [A2] and [A3].

The next step deals with the residual strength of the hull girder in the damaged condition. If the ship rests on the sea floor, further damage and additional hull girder loads may be caused by ebb tides and waves. This may in turn cause additional oil spill. Eventually, if the ship settles aground during a receding tide, the ship may split in half. Step (4) is dealt with in [A4].

After the hull damage is assessed, the grounding consequences may be established in terms of oil spill and flooding of compartments. This is done in step five (5), refer for instance Tavakoli et al. (2008). Finally, in step six (6) the consequences should be

evaluated against an acceptance criterion. This may be dealt with in a probabilistic manner. Step (5) and (6) are not treated in this thesis.

1.2.2 Scope of work

The scope of the work may be separated into different sub tasks. One part is dedicated to the relationship describing the indentation resistance of ship bottoms during stranding. This introduces several problems which need to be resolved. For instance, what is the typical sea floor condition? Because little is known about this prior to grounding, alternative methods for quantifying reasonable sea floor topologies are established. In the present work, the sea bed topology is categorized according to the type of structural damage it causes during a stranding event.

Apart from investigating the local stranding actions, a survey on the hull girder interaction is conducted. This implies that the hull girder loads are coupled to the sea floor contact forces, e.g. as the ship is lifted out of the water when subjected to tidal variations during stranding. Furthermore, the dynamic behavior of ships subjected to powered grounding is studied. This is done using a dynamic grounding code implemented by the author. This program calculates the ships external mechanics and combines this with simplified estimations of the contact forces.

A significant part of the work is devoted to estimation of fracture during grounding. It is key to capture this failure mode correctly. Not only is the capacity of ship structure in the action zone significantly reduced once fracture has occurred, but the ship also faces the risk of flooding and polluting the environment with fuel and cargo oil, as described in the initial introduction. The thesis is composed as follows:

Chapter 2 is based on information embedded in articles [A1] [A2] and [A3]. It gives an introduction to applied ductile fracture mechanics. Along with a short summary of existing fracture criteria applied in collision and grounding analyses of ships, a new criterion is presented. The chapter also summarizes the results from a series of panel indentation tests. These are further compared data generated from FEM simulations.

Chapter 3 deals with grounding of ships and contains elements from step 1-4 in the flow chart: Fig. 1.2. See also articles [A4] and [A5]. The damage effect caused by different sea floor geometries is studied. Further topics which are dealt with are: the external ship mechanics during powered grounding, and the hull girder interaction during stranding.

Chapter 4 contains the conclusions and summarizes the lessons learned. This chapter also discusses recommendations for future work.

Chapter 2

Modeling of fracture

This chapter deals with problems related to ductile fracture in ship structures, and gives a summary of articles [A1] to [A3]. A new and simple failure criterion is presented along with an already established criterion. In addition, the results from experimental and numerical analyses of panel indentation tests are presented.

2.1 Background

One of the main concerns in collision and grounding events is fracture in the outer hull and in cargo tanks. Once fracture occurs, the resistance to further damage drops dramatically. This may in turn accelerate the hull opening process. Potential consequences are; substantial oil spills and water flooding.

2.1.1 Material instability and ductile fracture

Ductile fracture is preceded by excessive plastic flow. In plate and shell structures this is often seen as excessive straining in narrow bands, characterized as local necks, see Fig. 2.1. Although, the material has not fractured at this stage, the event of local necking is severe. This is because a significant weakness appears in the material which is quickly followed by fracture.

Engineers have long investigated and attempted to understand the mechanisms behind local material instabilities. Keeler and Backhofen (1964) and Goodwin (1968) first mapped the formability of metals by constructing so called forming limit diagrams (FLDs). By applying loads in different directions on sheet metal, they observed that onset of local necking occurred differently for various load states, e.g. in uniaxial tension and biaxial tension. Physically, local necking can be described as a narrow band of material which starts to strain at a significantly higher rate than the surrounding material. The transition from uniform straining to local necking is

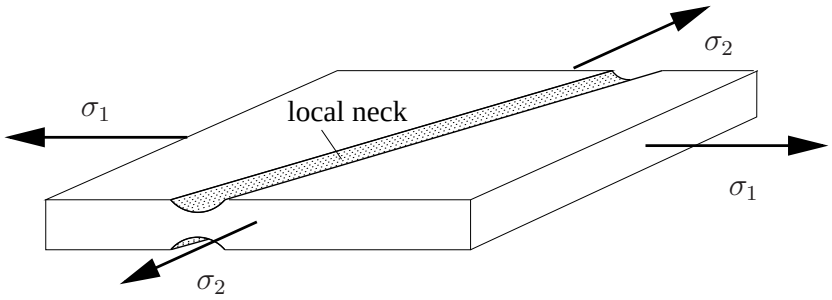

Figure 2.1: Development of a local neck in sheet metal. This is often referred to as a material instability and is quickly followed by ductile fracture.

often triggered by small imperfections or defects within the material. This observation has for instance been utilized by Marciniak and Kuczynski (1967) to formulate a procedure to predict local necking numerically.

Ductile fracture often occur shortly after the onset of local necking in sheet metal, and relates to the formation of micro-voids which grow and eventually coalesce as the material is strained. Such voids form at inclusions or hard second phases in regions which are highly deformed. The growth rate of these voids is controlled by the strain evolution and the hydrostatic stress state within the micro-structure. Studies on void growth within metal microstructure have, for instance, been conducted by McClintock (1968) and Rice and Tracey (1969). Eventually, as the voids coalesce and form small cracks, the material reaches a state where fracture is initiated, see Fig. 2.2. The importance of the hydrostatic stress state in ductile fracture mechanics has been investigated by Hancock and Mackenzie (1976) and Mackenzie et al. (1977).

The growth of micro-structural flaws and defects is in material modeling often associated with a damage variable D. The evolution of the material damage $\dot{D}$ is a way of describing the rate of void growth and has been used extensively by several authors, e.g. Lemaitre (1985),Bonora (1997), McClintock (1968) and Rice and Tracey (1969). The damage variable may either be coupled to the constitutive material laws or used separately as a local approach to determine the onset of fracture. Applied in a finite element code, the damage approach has proved a powerful tool to predict fracture in structures subjected to excessive straining.

Törnqvist (2003) gives a brief discussion on existing damage models and defines separate damage categories. These are void growth fracture criteria, continuum damage models (CDM), porosity based models and empirical criteria. Common for these is that the level of ductility changes with the state of hydrostatic stress.

Void growth criteria assume that the degree of void growth can be represented by a damage parameter D. Once this reaches a critical level, fracture is initi-

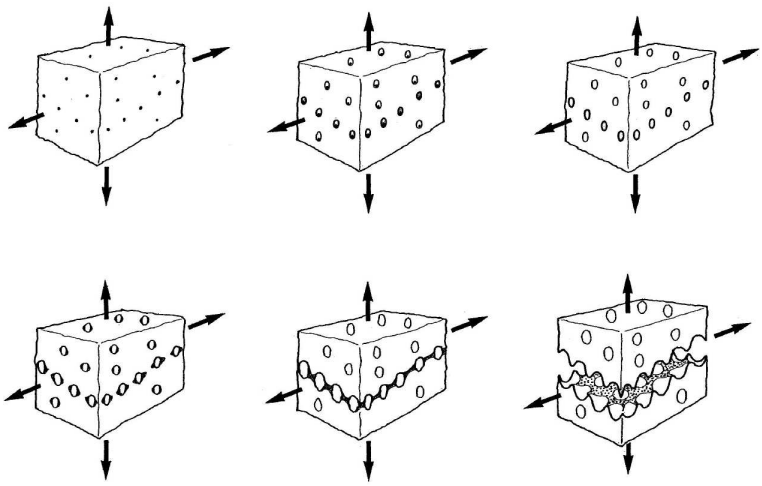

Figure 2.2: Void nucleation, growth and coalescence within the material microstructure.

ated. Examples on such criteria have been presented by McClintock (1968) and Rice and Tracey (1969). Continuum damage models (CDM) couple the constitutive material laws to the damage evolution $\dot{D}$. The material may in this way experience a degradation effect (softening) during plastic deformation. Fracture occurs once the damage D has reached a critical level. For further information on continuum damage models, refer Lemaitre (1985) and Bonora (1997). Finally, there are the porosity based models. As for CDMs, the porosity models also couple damage to the constitutive material laws. The difference lies in the way the material damage is defined. Porosity based models couple damage directly to the physics of void growth. CDMs, on the other hand, define damage as an evolution variable. The best known porosity based damage model is perhaps the Gurson (1975) model, which is found in many variants.

There are numerous empirical fracture criteria in use today. Most of them are simple criteria based critical stresses or strains. The most common of these is perhaps the equivalent plastic strain criterion. This criterion, however, has several flaws. The most significant is that fracture is predicted without the influence of the hydrostatic stress state. This is an over-simplification of fracture mechanics. A more refined empirical criterion may be described by the Cockcroft and Latham (1968) criterion.

2.1.2 Applied fracture criteria in collision and grounding analysis

Detailed analysis of ship collision and grounding requires information about the material properties. The material data available to the general engineer is, however, limited. Often the classification society only sets a minimum requirement to the steel grade. Furthermore, the sheer size of the ship often requires analyses with relatively coarsely meshed models. This is generally not united with a complex damage model. More pragmatic approaches are therefore required.

Törnqvist (2003) and Wang et al. (2006) presents summaries on existing fracture criteria developed for ship collision and grounding analysis. One such criterion is developed by Lehmann and Peschmann (2001). It is derived from strain measurements from large scale collision tests. The strains are recorded at crack faces as well as in more uniformly strained areas. The average strains are by Lehmann and Peschmann (2001) referred to as the "necking strain" ε_n (at crack faces) and the "uniform strain" ε_g (in less deformed areas), respectively. The criterion describes an equivalent plastic strain relationship which takes the mesh size sensitivity effect into account. This is formulated as

$$\varepsilon_{cr} = \varepsilon_g + \varepsilon_m \frac{x_e}{t} \frac{t}{l_e} \tag{2.1}$$

where l_e is the element length and, t is the element thickness and x_e describes the average width of the local necks measured at the crack faces. Lehmann and Peschmann (2001) have reported that $\varepsilon_m \frac{x_e}{t}$ can be condensed into a single parameter denoted α. For plate thicknesses in the range of 5 -12 mm, the material parameters (ε_g, α) have values equal to 0.1 and 0.8, respectively. For thicker plates (12 mm and above), $\varepsilon_g = 0.08$ and $\alpha = 0.65$.

A similar rationale is applied by Germanischer Lloyd (GL) to derive a fracture criterion based on plate thinning. As with the Peschmann criterion, this criterion also varies with the element size. The available documentation on this criterion is limited. A short description can nevertheless be found in the article presented by Zhang et al. (2004). The criterion is expressed as

$$\varepsilon_{cr}^t = \varepsilon_g^t + \varepsilon_e^t \frac{t}{l_e} \tag{2.2}$$

where ε_g^t and ε_e^t denotes the uniform and the ultimate strain in the thickness direction, respectively. The default values for these are 0.056 and 0.54, respectively. Both the Peschmann criterion and the GL criterion are further investigated and discussed by Ehlers et al. (2008). In the cases that were studied, the Peschmann criterion seemed to give the most reliable results, although no recommendation on which criterion to use is given.

A recent criterion which includes the influence of hydrostatic stresses is presented by Lehmann and Yu (1998). This is referred to as the rupture index I_R, and is expressed by

$$I_R = f\left(\frac{\sigma_m}{\sigma_{eq}}\right)^m \varepsilon_{cr} \tag{2.3}$$

where ε_{cr} is the equivalent strain at fracture and $m = 2n+1$, describes a material parameter which depends on the power law exponent n. The power law expresses the material stress-strain relationship. This is given as $\sigma_{eq} = K\varepsilon_{eq}^n$. Here (K, n) are material parameters and $(\sigma_{eq}, \varepsilon_{eq})$ denote the equivalent stress and plastic strain, respectively. The rupture index incorporates a hydrostatic stress dependency. This is accounted for by the triaxiality function which is derived from the Lemaitre (1985) continuum damage model

$$f\left(\frac{\sigma_m}{\sigma_{eq}}\right) = \frac{2}{3}(1+\nu) + 3(1-2\nu)\left(\frac{\sigma_m}{\sigma_{eq}}\right)^2 \tag{2.4}$$

where ν is the linear elastic Poisson factor. The rupture index is calibrated from uniaxial tensile tests. Once this criterion passes a critical level, fracture is initiated. Broekhuijsen (2003) has applied this criterion with success to calculate the fracture resistance of 12 mm steel specimens.

2.2 Applied fracture criteria

Two failure criteria are applied in this thesis. The first one is the so called Rice-Tracey-Cockcroft-Latham criterion (RTCL) which is presented in details by Törnqvist (2003). The second is the Bressan-Williams-Hill (BWH) instability criterion, see [A1]. The criteria are along with material sub routines implemented into LS-DYNA.

The material subroutines are based on von Mises theory (J_2) and uses a modified power law relation to describe the material stress strain curve, see [A1]. In order to return to the yield surface when operating in the plastic regime, two types of algorithms have been applied. These are the so called cutting plane algorithm and the closest point projection algorithm. Refer for instance Belytschko et al. (2004), Crisfield (1997), Skallerud and Amdahl (2002) and Ortiz and Simo (1986) for a detailed description. Both methods return to the yield surface with a quadratic convergence rate. Little or no difference in the simulations between these two methods is therefore discovered. Considering the short time steps applied in explicit FE simulations and acknowledging the fact that most simulations are performed quasi-statically, a satisfactory return is usually achieved within a few (1-3) iterations. Plane stress conditions for shell elements are enforced directly by using plane

stress tensors, see Crisfield (1997). Similar versions of plane stress return mapping algorithms are described by Jetteur (1986) and Simo and Taylor (1986).

2.2.1 The RTCL damage criterion

The RTCL damage criterion describes a combined Rice and Tracey (1969) damage criterion and modified Cockcroft and Latham (1968) damage criterion. These criteria are both dependent on the hydrostatic stress state, which in the following is normalized by the equivalent stress. This gives the well known expression for the triaxial stress state $T = \frac{\sigma_m}{\sigma_{eq}}$. Here σ_m is the hydrostatic stress and σ_{eq} is the equivalent stress. The RTCL criterion describes an accumulating damage D, which is expressed by the evolution rule

$$\dot{D} = \begin{cases} 0 & \text{if } \ T < -1/3 \\ \frac{\sigma_1}{\sigma_{eq}}\dot{\varepsilon}_{eq} & \text{if } \ -1/3 \leq T < 1/3 \\ \exp\left(\frac{3T-1}{2}\right)\dot{\varepsilon}_{eq} & \text{otherwise} \end{cases} \tag{2.5}$$

where $\dot{D}$ denotes the rate of damage, σ_1 is the major principal stress and $\dot{\varepsilon}_{eq}$ is the rate of the equivalent plastic strain. Fracture is initiated once the accumulated damage reaches a critical level. An important feature with this criterion is that for proportional loading in uniaxial tension ($T = 0.33$), the damage evolution $\dot{D}$ is exactly matched by rate of equivalent plastic strain $\dot{\varepsilon}_{eq}$. This is convenient with respect to calibration, because the critical damage D_{cr} most easily can be found from uniaxial tensile tests. From this a normalized criterion can be expressed

$$D = \frac{1}{\varepsilon_{cr}} \int \dot{D} dt \tag{2.6}$$

where ε_{cr} is the critical equivalent plastic strain in uniaxial tension. In this form, failure will appear once the damage D approaches the value of one.

In the thesis, the RTCL criterion is used with shell elements. However, void growth is in reality a three dimensional process. Consequently, in order model fracture initiation in the best possible way, through-thickness "crack growth" is described as a loss of resistance and stiffness in each through-thickness integration point. The elements are removed once all integration satisfies the following condition $D > D_{cr}$. A more detailed presentation of the RTCL criterion is given by Törnqvist (2003)

2.2.2 The BWH instability criterion

In accidental analysis of large scale shell structures, it may be well worth considering the onset of local necking as a state of failure, rather than searching for fracture after

local necking. There are three reasons for this. First, the evolution of local necks can not be followed with coarse shell elements. Second, the hydrostatic stress state at the location of the local neck changes once the instability initiates, see Atkins (1996). Also this effect can not be captured by large elements. Finally, in the simplest form, the onset of instability can be determined analytically, based on the shape of the material stress-strain curve. This simplifies calibration and gives a pragmatic criterion.

The BWH criterion describes a simplified way of determining the onset of local necking. It describes an analytical forming limit in the stress space, and is therefore not limited to proportional strain paths. See for instance Stoughton (2000), Stoughton (2001) and Stoughton and Zhu (2004). The BWH instability criterion combines local necking analysis presented by Hill (1952) with the Bressan and Williams (1983) shear stress criterion. In its original form, the Hill criterion assumes that a local neck will form with an angle ϕ to the major principal stress direction. Within this neck, the strain increments along the narrow necking band will be zero. Consequently, the cross section of the neck will be subjected to plane straining. The orientation of the local neck may be expressed as

$$\phi = \tan^{-1}(\sqrt{-1/\beta}) \tag{2.7}$$

where β describes the degree of biaxial straining, $\beta = \dot{\varepsilon}_2/\dot{\varepsilon}_1$, and $\dot{\varepsilon}_1$ and $\dot{\varepsilon}_2$ are the major and minor principal strain rates, see Fig. 2.3. This yields rational results only for negative values of β. It is worth noticing that there is a direct relationship between the stress triaxiality T and β. For the plane stress condition when elastic strains are neglected this yields

$$T = \frac{1}{\sqrt{3}} \frac{\beta + 1}{\sqrt{\beta^2 + \beta + 1}} \tag{2.8}$$

At the instant a local neck is formed, the effects from strain hardening and the diminution in thickness balance each other exactly. This implies that the tractions within the material reach a maximum value at the point of local necking. From these assumptions the following condition for onset of local necking in metal sheets may be derived.

$$\frac{\dot{\sigma}_1}{\dot{\varepsilon}_1} = \sigma_1(1 + \beta) \tag{2.9}$$

where σ_1 and $\dot{\sigma}_1$ are the major principal stress and stress rate. Assuming power law strain hardening, and that the stress rate ratio $\frac{\dot{\sigma}_2}{\dot{\sigma}_1}$ at the point of instability equals the stress ratio $\frac{\sigma_2}{\sigma_1}$, the following expression for Hill's criterion emerges

$$\sigma_1 = \frac{2K}{\sqrt{3}} \frac{1 + \frac{1}{2}\beta}{\sqrt{\beta^2 + \beta + 1}} \left(\frac{2}{\sqrt{3}} \frac{n}{1 + \beta} \sqrt{\beta^2 + \beta + 1} \right)^n \tag{2.10}$$

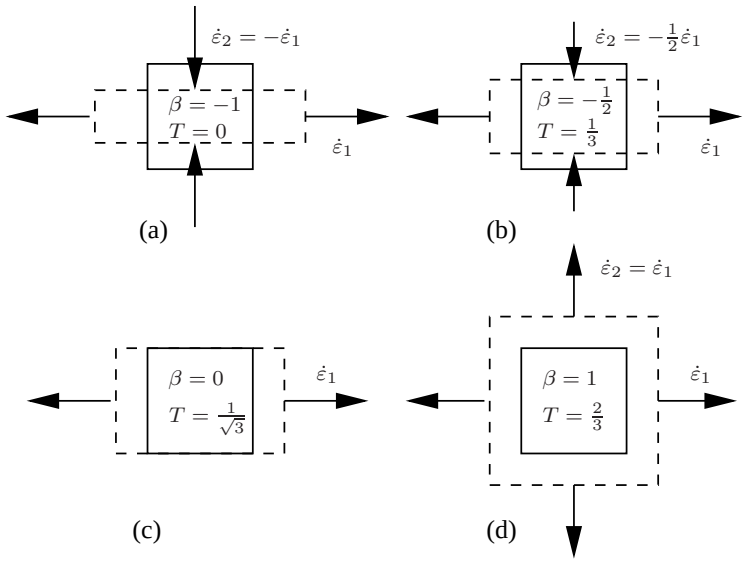

Figure 2.3: Strain states in terms of the strain rate biaxiality β and the stress triaxiality T. All conditions refer to a plane stress state: (a) shows a pure shear state, (b) refers to uniaxial tension, (c) illustrates plane straining, and (d) shows equi-biaxial stretching.

where (K, n) are power law parameters. Stoughton and Zhu (2004) have presented a similar stress based Hill formulation. According to Eq. (2.7), Hill's analysis is only valid for negative values of β. In the positive regime, the Bressan-Williams shear stress instability criterion is used. It states: The instability in a sheet element is initiated once a critical shear stress is reached in a direction inclined through the thickness at which the sheet element experiences no change in length. This gives the following expression for the critical major principal stress

$$\sigma_1 = \frac{2\tau_{cr}}{\sqrt{1 - (\frac{\beta}{2+\beta})^2}} \tag{2.11}$$

where the critical shear stress is matched by the Hill criterion when $\beta = 0$. This gives

$$\tau_{cr} = \frac{1}{\sqrt{3}} K (\frac{2}{\sqrt{3}} n)^n \tag{2.12}$$

By combining the Hill criterion with the Bressan-Williams criterion, the following

expression is established

$$\sigma_1 = \begin{cases} \frac{2K}{\sqrt{3}} \frac{1+\frac{1}{2}\beta}{\sqrt{\beta^2+\beta+1}} \left(\frac{2}{\sqrt{3}} \frac{n}{1+\beta} \sqrt{\beta^2+\beta+1} \right)^n & \text{if } \beta \leq 0 \\ \frac{2K}{\sqrt{3}} \frac{(\frac{2}{\sqrt{3}}n)^n}{\sqrt{1-(\frac{\beta}{2+\beta})^2}} & \text{otherwise} \end{cases} \tag{2.13}$$

Because the BWH criterion searches for local instability, it applies to membrane stresses and strains only. The effect of bending is left out. When applied in a finite element code, this is achieved by searching for violation of the instability criterion only in the mid through-thickness integration point of every shell element. Once the criterion is violated, the element is removed and fracture is initiated. The BWH criterion is presented in details in [A1] and is verified analytically and numerically against experimental data found in literature.

2.2.3 Accounting for element size sensitivity

The finite element method is sensitive to the element discretization at large deformations. A fine mesh may for instance indicate strain concentrations at certain locations. This may not be captured by a coarser mesh. The effect is especially apparent close to crack tips, at structural intersections, or in post necking zones. Shell elements are especially sensitive to stress and strain consentrations. This is due to the plane stress formulation which gives little through-thickness resistance. While through thickness stresses stabilizes solid elements subjected to thinning, shell elements are only restrained by neighboring elements in terms of in-plane compatibility. Consequently, close to failure, shell elements are free to deform in the thickness direction and may strain excessively in narrow bands as wide as the element itself. This effect is especially seen when small elements are used. When large elements are applied, the problem is rather that strain concentrations remain uncaptured. Preventive measures are therefore needed in order to minimize this effect.

The element size used in analyses of collision and grounding is often found in the range of 5-10 times the sheet thickness. Material instability, on the other hand, typically takes place in narrow bands. The width of these are typically in the order of the sheet thickness, see Hosford and Caddell (1993) and Wang et al. (2007). Obviously, such local mechanisms can not be captured in collision and grounding analyses. Several authors have accounted for this discrepancy by making the fracture criterion vary with the element size, see for instance Törnqvist (2003) and Ehlers et al. (2008). Basically, this implies that the failure strain or damage is scaled to a lower level in order to simulate onset of fracture at the correct indentation and internal energy level. In this way, the total strain energy at fracture will ideally be similar for all mesh sizes.

Derivation of a element size dependent "failure scaling law" is made in [A3]. This scaling law assumes that strain localizations occur within large elements at the point of fracture, see Fig. 2.4. In uniaxial tension the scaling law can be expressed as

$$\varepsilon_{cr} = n + (\varepsilon_n - n)\frac{t}{l_e} \tag{2.14}$$

where n is the power law exponent and (t, l_e) are the element thickness and characteristic length, respectively . The average failure strain within the local neck, ε_n, may be found from simulations of tensile tests. This expression can be used to calibrate the RTCL criterion, Eq. (2.6). It is implemented by the author into LS-DYNA, as a fully automated function. It should, however, be mentioned that expressing the failure strain as a function of the element size may be dangerous. It is not guaranteed that strains localize prior to fracture. Applying formulations as given by Eq. (2.14) should therefore be made with caution.

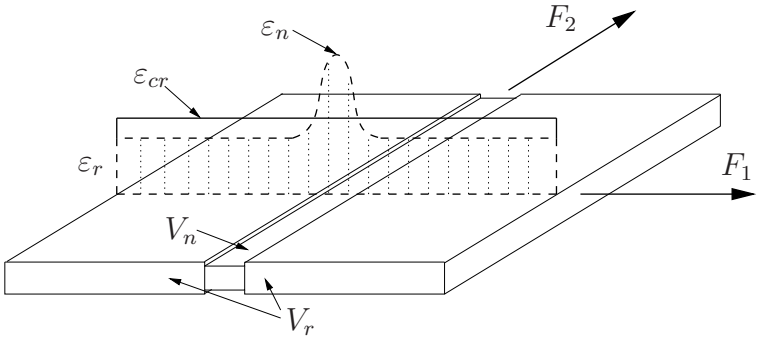

Figure 2.4: Simplified illustration of the procedure to generate the critical strain ε_{cr} for an element. The constant critical strain, ε_{cr}, is the volume weighted result of an assumed internal element strain distribution. ε_r and ε_n indicate the average strain values outside the and inside the strain localization, respectively. F_1 and F_2 represent element tractions.

2.3 Indentation of stiffened panels

The BWH and the RTCL criterion have been applied in simulations of laboratory tests. The experiments and simulations are presented in [A2 – A3].

2.3.1 Plate indentation experiments

A series of plate indentation tests have been carried out in order to study the response of double bottom panels subjected to grounding actions. Each of the spec-

imens are indented by a conical model of the sea floor, see Fig. 2.5. This is in the following referred to as an "indenter". It is assumed that the experiments represent idealized stranding scenarios, where only the panel section between the girder webs is subjected to deformation.

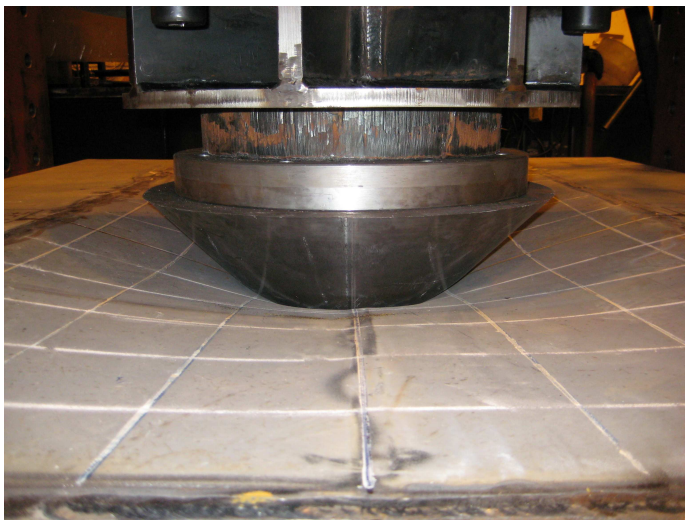

Figure 2.5: The experiment. The indenter forces the panel to deform.

Five specimens have been tested. They share the same plate geometry, but have different stiffener configurations. Both flat bar (FB) stiffeners and bulb (HP) stiffeners are applied to the models. The specimens are found in single and paired stiffener configurations. The panels are indented to and beyond the point of fracture. The panels are illustrated in Fig. 2.6. A detailed description of the tests is given in [A2].

2.3.2 Experiment motivation, observations and discussions

The tests have been carried out for two reasons: They allow a closer investigation of the resistance to indentation of various hull panel configurations. Second, experimental data for numerical verification of the fracture criteria are generated.

The force-indentation relationship for each test is plotted in Fig. 2.7. All experiments show consistently that introducing large stiffeners in hull panels, yields stiffer and less flexible structure. This in turn introduces more localized deformations and thus, earlier fracture. It may therefore be concluded that in order to achieve a "ductile design", weaker stiffeners are required. The danger by pursuing this rationale is that the structure may become too weak and wobbly to fulfill its normal operational requirements. The solution to this may be found in alternative designs, where massive stiffeners are omitted. See for instance the Sandwiched-Polymer-

(a)

(b)

(c)

(d)

(e)

(f)

Figure 2.6: Indentation of steel panels. Figure (a) shows the unstiffened plate prior to fracture, and (b) after fracture. Figure (c) and (d) correspond to the indentation of a panels with one flat bar stiffener before and after fracture, respectively. Figure (e) and (f) illustrate the response of a plate with two flat bar stiffeners.

Structure (SPS) presented by Brooking and Kennedy (September 2004), and the Y-core double bottom and side structure presented van de Graaf et al. (2004). A

similar philosophy is also presented by Tautz (2007). By applying intentional failure points between stiff frame sections and cargo tanks, the tank plating is designed to release from the transverse frames during a collision event. In this way, deformations are spread over a larger zone, which may prevent penetration.

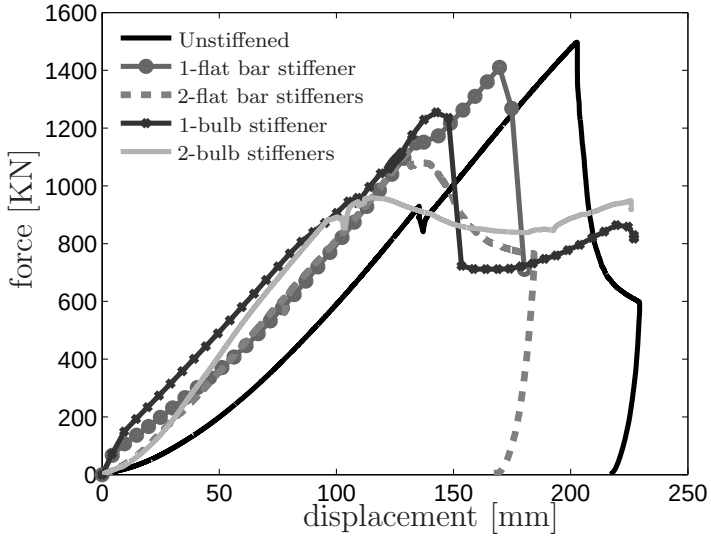

Figure 2.7: Force-indentation curves for the various tests.

Another and important observation made in the tests, is that panels are capable of redistributing loads after penetration. Especially the panels with two stiffeners shows this behavior, see Fig. 2.7.

2.3.3 Finite element simulations

The FE simulations of the tests are conducted as described in [A3]. Each model is simulated using three different element sizes. These range from 1 to 4 times the sheet thickness. Both the BWH and the RTCL criteria are applied in the analyses. Because the RTCL criterion predicts fracture at the final stage of deformation, e.g. after local necking, it is scaled as a function of the element size, see Eq. (2.14). This implies that large elements should fail at a lower strain value than small elements. As explained earlier, this is done to achieve failure at the same deformation regardless of the mesh size. The same scaling has not been applied with the BWH criterion. This is because fracture is initiated once onset of local necking is detected. In theory this implies that the criterion avoids strain concentrations which are established by local necks.

Figure 2.8 shows the equivalent strain distribution in the unstiffened panel prior to fracture. The strains at this stage are fairly smoothly distributed and show no tendency of localization. This is also confirmed from observations made in the test.

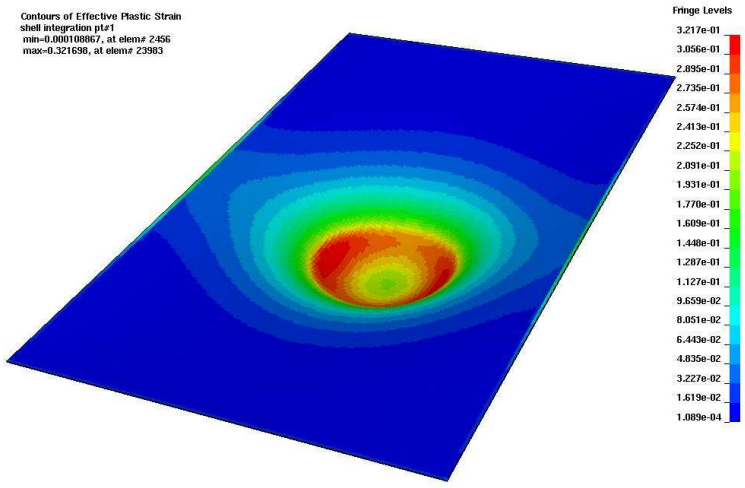

Figure 2.8: Indentation of the unstiffened panel. The color distribution illustrates the degree of equivalent plastic straining.

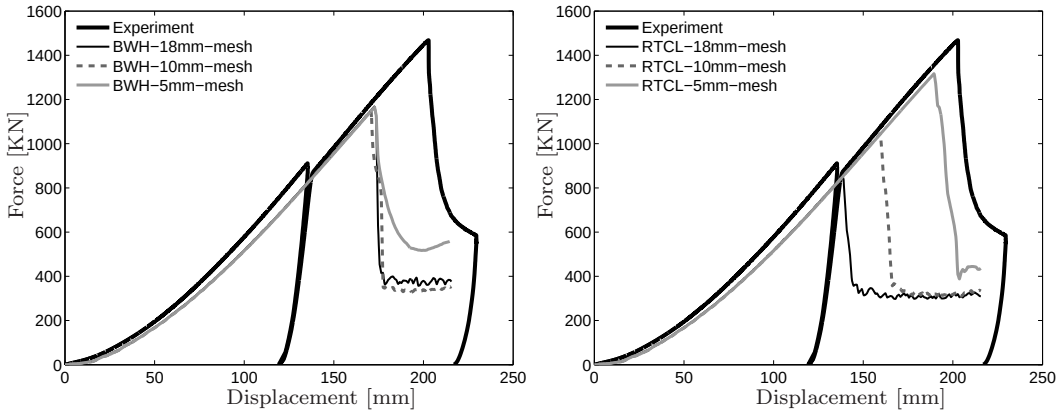

Figure 2.9: Force-indentation behavior of the unstiffened plate. Figure (a) shows simulation results achieved using the BWH criterion (without failure scaling), and (b) shows results using the RTCL criterion (with failure scaling).

Figure 2.9 shows the calculated results using both the BWH (a) and the RTCL

(b) criterion. Because strains in this case do not consentrate prior to fracture, using a failure scaling law should be avoided. This is confirmed by the scatter which is produced by using the RTCL criterion scaled by Eq. (2.14). The unscaled BWH criterion produces no such inconsistency.

2.3.4 Mesh sensitivity - proposal

Although the formulation of the BWH criterion yields less mesh sensitive results than ordinary damage criteria, the element size effect is not escaped entirely. This is especially the case for FE models which have structural intersections and sharp corners. This gives stress and strain concentrations, which will be captured differently by various element sizes. Consequently, all fracture criteria will show some sensitivity to the mesh discretization. Counter actions are therefore needed.

When small shell elements are applied, the concern is excessive straining in local zones. Again, this is attributed to the lack of through thickness resistance in shell elements. A reduction in mesh sensitivity may, however, be achieved by adding smoother transitions between structural intersections. This may for instance be achieved by introducing element rows which represent welds, see [A3]. If elements smaller than the plate thickness are applied, one might also concider using "non-local methods" to control the thinning process, see Wang et al. (2007).

The most common way to deal with the mesh sensitivity is to introduce an element size "scaling law", e.g. Eq. (2.14). Simulations of the unstiffened panel shows, nevertheless, that this may be dangerous. By scaling the failure strain, it is explicitly assumed that a localization will take part in the strain field prior to fracture. As discussed, such strain concentrations may in reality not appear. Thus, scaling laws need restrictions. It is observed in [A3] that strain concentrations appear close to changes in the structural geometry, e.g. structural intersections, crack tips and sharp corners. It is therefore reasonable to restrict application of Eq. (2.14) to such locations, only. Enforcing this restriction may be done during pre-processing by running simple programs which read the finite element input file, recognize all nodes shared by more than four elements (Q4 shell elements), and write an updated FE input file. In this file, elements at structural intersections have scaled failure properties. If applied with the BWH criterion, the scaling law must be incorporated into the BWH expression. According to [A3] the element size dependent BWH criterion can be expressed as

$$\sigma_1 = \begin{cases} \frac{2K}{\sqrt{3}} \frac{1+\frac{1}{2}\beta}{\sqrt{\beta^2+\beta+1}} \left(\frac{1}{\sqrt{3}} \frac{n(\frac{t}{l_e}+1)}{1+\beta} \sqrt{\beta^2+\beta+1} \right)^n & \text{if } \beta \leq 0 \\ \frac{2K}{\sqrt{3}} \frac{\left(\frac{1}{\sqrt{3}} n(\frac{t}{l_e}+1) \right)^n}{\sqrt{1-(\frac{\beta}{2+\beta})^2}} & \text{otherwise} \end{cases} \tag{2.15}$$

As previously, no external input parameters are needed. The RTCL criterion can be scaled, at structural intersections, as previously. This procedure is illustrated through analyses of the stiffened panels in Fig. 2.10.

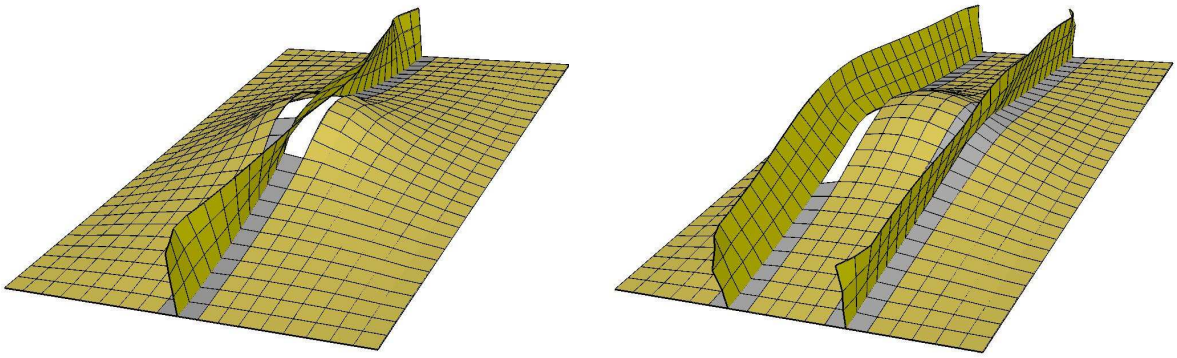

(a) (b)

Figure 2.10: Simulations of (a), panel 1-FB and (b), specimen 2-FB. The scaling law Eq. (2.14) is only applied to the plate-stiffener intersection. The characteristic element size is equal to 8 times the plate thickness.

The simulations results are shown in Fig. 2.11. Figure (a) and (b) refer to simulations of the specimen with one stiffener, refer Fig. 2.10 (a). Figure (c) and (d) refer to simulations of the specimen with two flat bar stiffeners. In all cases, three models with different mesh sizes are applied.

The results achieved with the location controlled scaling law is in general good. Both the BWH and the RTCL criterion now manages to initiate fracture at the correct location. In turn, this gives force-indentation relationships which agrees well with the experiments.

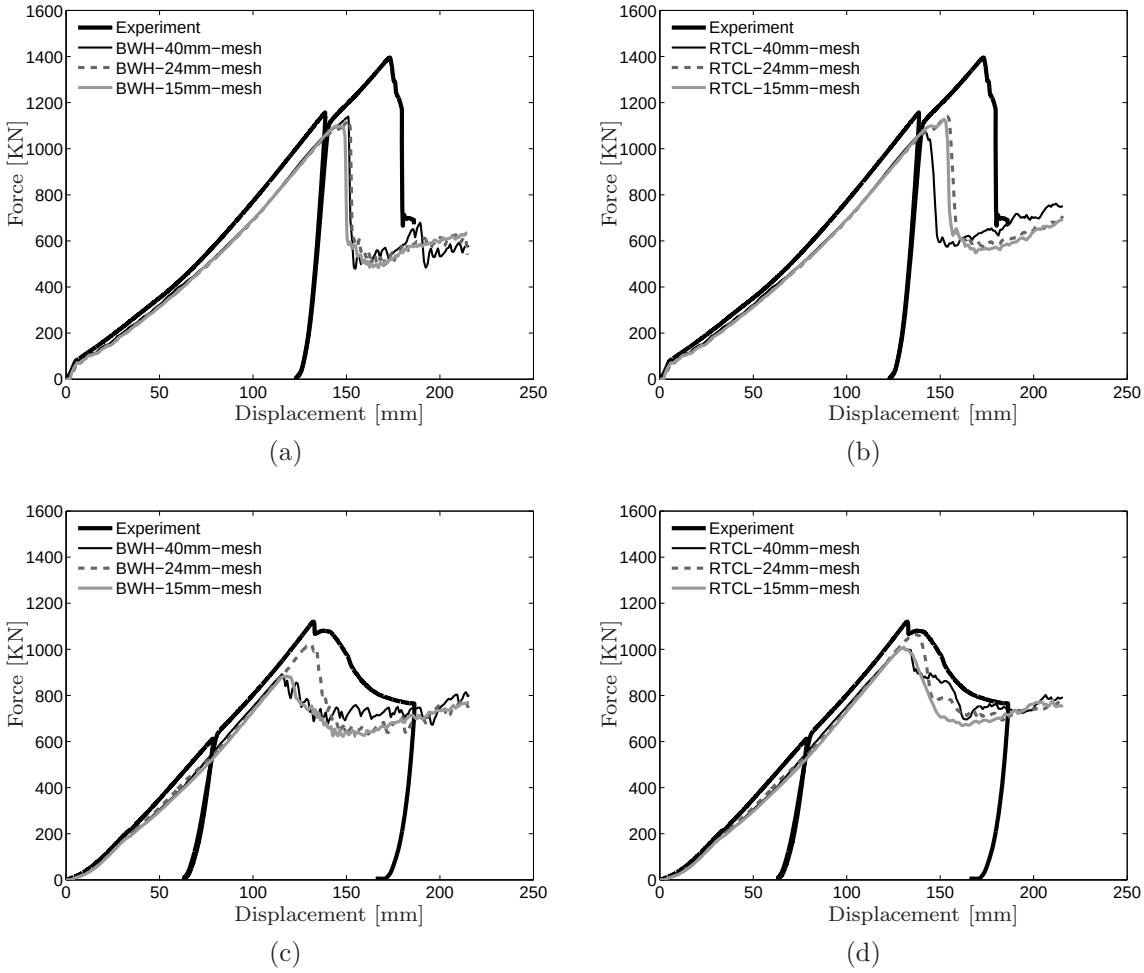

Figure 2.11: Simulated indentation force of panels with one and two flat bar stiffeners, see (a) (b), and (c) (d), respectively. Figure (a) and (c) are generated with the BWH criterion and, (b) and (c) are generated using the RTCL criterion. Only the element row next to stiffeners are subjected to (failure) scaling.

2.4 The Amdahl and Kavlie double bottom indentation tests

Amdahl and Kavlie (1992) have reported results from two double bottom crushing tests. The structures were assembled by welding and the double bottom boundaries were kept fixed by massive frames. The experiments were carried out using the same hydraulic jack as used in the panel indentation tests. The double bottom arrangement is illustrated in Fig. 2.12.

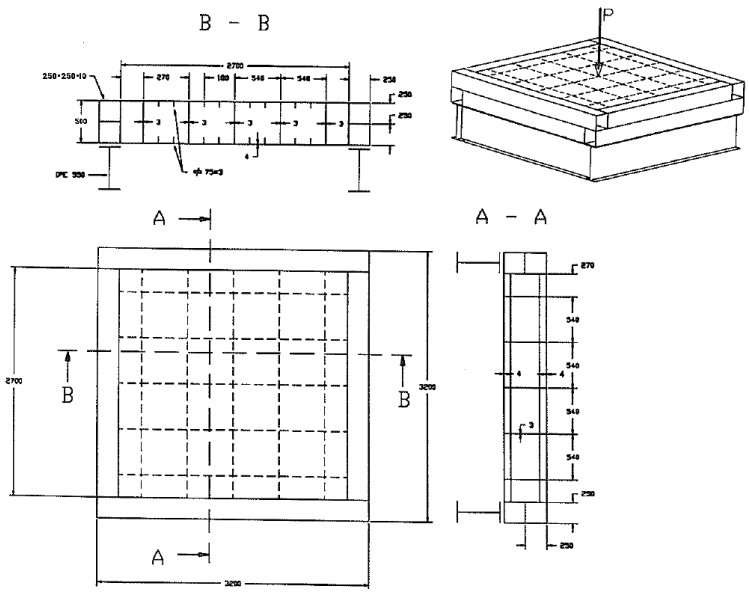

Figure 2.12: The dimensions of the double bottom stranding test.

2.4.1 The finite element model

Three different mesh sizes have been applied in this investigation. These are the same ones as reported in Alsos and Amdahl (2007c), namely 20 mm, 14 mm and 8 mm mesh. In all cases Belytsckho-Lin-Tsay shell elements with five through-thickness integration points are applied. The indenter is modeled as a truncated cone with a 55 degree apex angle. This coincides well with the true indenter and the indenter geometry reported by Törnqvist (2003).

The tests specimen was fabricated in grade A mild steel with yield stresses equal to 330 MPa. In the following, the material properties are modeled using a modified power law stress-strain relationship, see [A1] and [A3]. This formulation includes

the plateau strain and yields

$$\sigma_{eq} = \begin{cases} \sigma_Y & \text{if } \varepsilon_{eq} \leq \varepsilon_{plat} \\ K(\varepsilon_{eq} + \varepsilon_0)^n & \text{otherwise} \end{cases} \tag{2.16}$$

where ε_{plat} is the equivalent plastic strain at the plateau exit and σ_Y is the initial yield stress. The strain ε_0 describes an expression which allows the plateau and power law expression to intersect at $(\varepsilon_{plat}, \sigma_Y)$. This is given as

$$\varepsilon_0 = \left(\frac{\sigma_Y}{K}\right)^{\frac{1}{n}} - \varepsilon_{plat} \tag{2.17}$$

The power law data are extracted from nominal material data presented by Amdahl and Kavlie (1992) and are illustrated in table 2.1

Table 2.1: Powerlaw material parameters for the structural components.

Specimen	σ_Y [MPa]	K [MPa]	n	ε_{plat}
Bottom plating	330	755	0.190	0.015
Girder webs	330	790	0.180	0.005
Stiffeners	330	740	0.205	0.022

It might be argued that the restriction of the failure scaling law, Eq. (2.14), applied in section 2.3.4 becomes self enforcing when analyzing large scale grounding or collision scenarios. Stiff girders and frames have a way of introducing excessive deformation in intersecting panels. Fracture may therefore appear at these locations without any additional restrictions to the failure scaling law. This is assumed in the following.

2.4.2 Results and discussion

The results of the simulation are shown in Fig. 2.13. The agreement between numerical and experimental results is good. The effect of changing the mesh is small. Some discrepancies are observed, though. The simulations indicate fracture at a load level between 1300 - 1500 KN rather than 1200 KN as in the experiment. This may be explained by that the experiment had inadequately fabricated joints, and the fact that not all stiffeners had continuous welds, Gjerstad (1992). Simulations with the RTCL criterion performed by Törnqvist (2003) show the same behavior as here. This indicates that the poor properties of the welds may have had a significant impact on the test response.

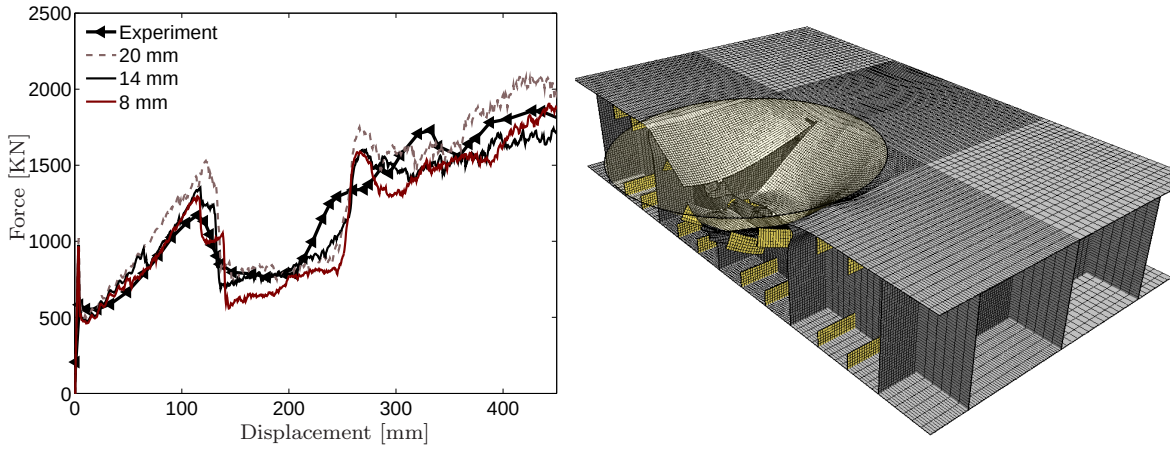

(a) (b)

Figure 2.13: Simulations of the Amdahl and Kavlie double bottom stranding test. Figure (a) shows the force-indentation relationship, while (b) shows the penetrated FE model.

An interesting observation is that fracture in all simulations take place at plate-stiffener and plate-girder web intersections. This is in accordance with the scaling restriction applied in section 2.3.4, although in this case it is self enforced. The excessive straining close to plate-girder intersections create strain concentrations which are detectable even for large elements. If fracture on the other hand appears outside the intersection areas, there is reason to be suspicious. The procedure described in section 2.3.4 is therefore preferred.

Chapter 3

Finite element analysis of ship grounding

This chapter deals with grounding of ships and discusses the consequences of different grounding scenarios. The work is described in details in [A4–A5].

3.1 Grounding scenarios

Ships subjected to grounding often suffer severe damage. The deformation pattern depends heavily on the grounding scenario. The shape of the sea floor is obviously an important factor. For instance, grounding on sharp obstacles provokes different grounding damage than grounding on sand banks. The same holds true for stranding versus dynamic grounding.

Although the sea floor topology plays a governing role during grounding, little information is available about this in the literature. Up to the present, ships are typically assumed to run aground on sharp obstacles such as wedges or pinnacles. Obviously this is inspired by high profile accidents such as the "*Exxon Valdez* " accident. Such scenarios involve tearing and puncturing of cargo tanks. However, limiting analyses only to raking scenarios is insufficient. Consider for instance the "*Prestige*" accident. Rather than grounding with forward speed on a sharp pinnacle, it split in half at sea. The result was an environmental disaster. This shows in a convincing way that scenarios where the global hull girder capacity is affected may be as severe as raking scenarios. Wider investigations are therefore necessary in order to map the severity of different grounding scenarios.

Wang et al. (2000) have presented a study on the behavior of double bottom sections subjected to grounding actions. By conducting indentation tests on scaled down specimens using different indenters, the structural behavior was recorded for various grounding scenarios. The trend from the tests shows that large indenters

require far more energy to fracture the shell plating than small indenters.

The sea floor shape and size has in the following been categorized into three groups. The requirements for these groups have been set by a reverse approach to identify characteristic sea floor "properties", see [A4]. Rather than conducting direct bottom roughness surveys, the sea floor is characterized according to the type of hull damage which occurs during grounding. This is calculated numerically in LS-DYNA for a tanker section. As presented in [A4], this gives basis for the following sea floor categories, see Fig. 3.1:

1. "Rock": The *rock* describes a sharp geometry which during grounding puts concentrated loads on the ship bottom. This in turn, leads to early fracture/penetration and localized structural damage.

2. "Shoal": The *shoal* describes a large sea floor geometry. This may cover the whole ship breadth. Large parts of the ship may get damaged during grounding, although penetration is less likely. Due to an extensive contact surface, large forces must be expected.

3. "Reef": The *reef* describes an intermediate sea floor obstruction. In this case it is not so easy to see the response of the double bottom apriory in terms of local or global deformations.

These sea floor conditions are applied in finite element simulations of tanker stranding. In total 12 different scenarios are analyzed, see [A4].

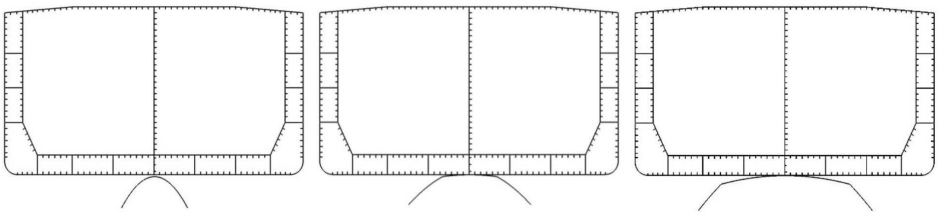

Figure 3.1: Sea floor conditions. Grounding on a rock, reef and shoal.

3.2 Grounding damage and resistance

The resistance to indentation and the subsequent hull girder damage caused by grounding is studied in details in [A4] and [A5]. In both papers, a shuttle tanker

holding a displacement of 140,000 m^3 is assumed to either run aground or strand during a receding tide. The internal arrangement of the ship is illustrated in Fig. 3.2

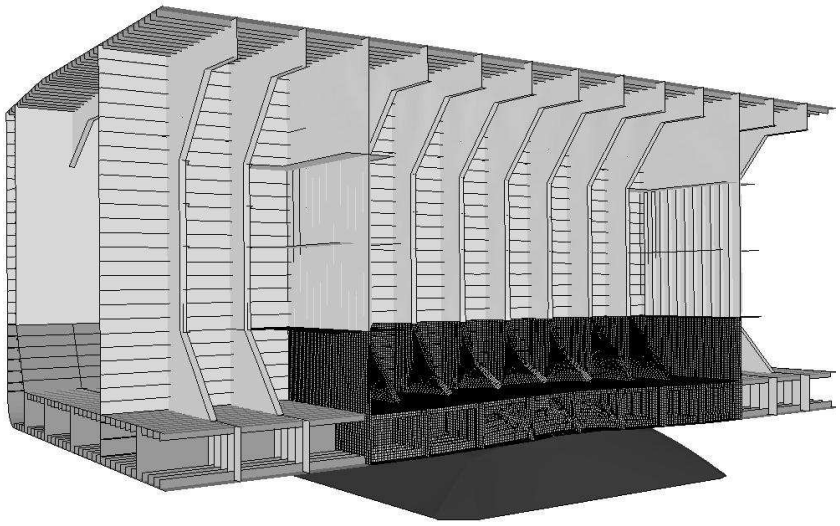

Figure 3.2: Finite element model of a shuttle tanker subjected to stranding.

3.2.1 Stranding - double bottom indentation

The behavior of the double bottom due to stranding on rocks and shoals is illustrated in Fig. 3.3. Stranding on a rock involve local damage and early hull penetration. Fracture is even recorded in the cargo tank. Obviously this kind of damage is critical with respect to oil spill. Figure 3.3 (b) illustrates grounding on a shoal. In this case the dominating mode of energy absorption comes from crushing and grillage deformation of the girder webs. The large contact area introduces little strain concentrations in the inner and outer hull plating. Hence, the simulations show no indication of initiating fracture in the outer shell. Cargo tank penetration is therefore not a main concern. A more critical issue is the generation of hull girder bending moments, e.g. consider stranding amidship during a receding tide.

The grounding contact forces are plotted in Fig. 3.4. The scenarios 1-4 refer to various contact locations. For instance, location 1 and 2 indicate contact directly on the cargo tanks. Scenario 3-4 represent contact at the longitudinal bulkhead, see [A4] for the detailed description. In the case of stranding on a rock, the maximum resistance is reached at approximately 60-70 MN. This occurs once the cargo tank is penetrated. This level corresponds to 4-5% of the total ship displacement. If stranded amidship, and assuming poin load grounding actions, this corresponds to

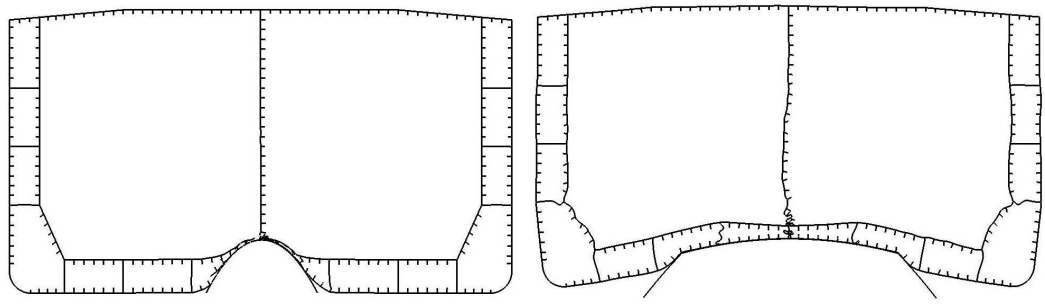

(a) (b)

Figure 3.3: Cross section of the tanker hull. Figure (a) shows damage due to stranding on a rock while (b) shows damage due to grounding on a shoal.

a 0.6 m hull girder out of the water displacement and a 2000 MNm hogging moment. In comparison the still water rule requirement is 4100 MNm. This indicates that the global hull girder response and the local bottom damage can be treated seperately. Grounding amidships on a shoal, on the other hand, yields a maximum resistance in the range of 250-300 MN. This corresponds to 20% of the ships total weight. Surely, there will be an interaction between contact forces and global hull girder bending moments at this stage. The ship may split in half during this scenario. Hence, it investigated in details later in the thesis.

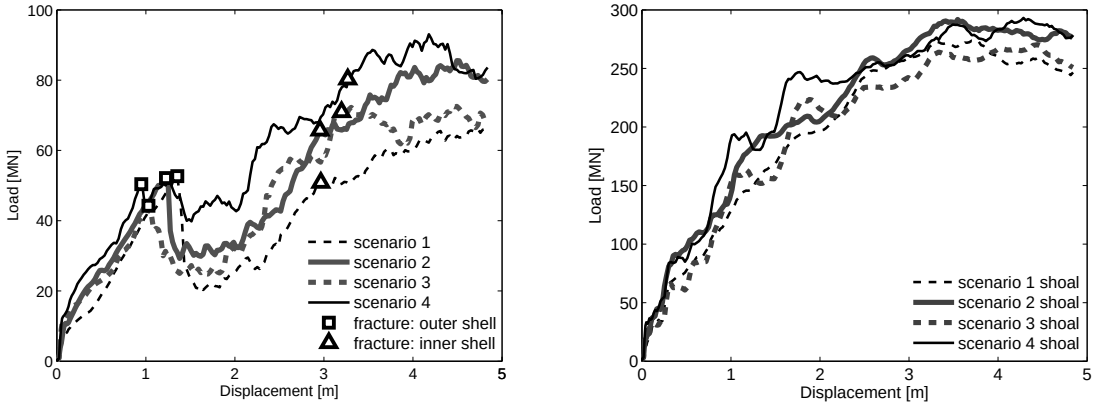

(a) (b)

Figure 3.4: Contact forces during stranding. Figure (a) shows the force indentation curve during stranding on a rock, while Fig. (b) shows contact forces during stranding on a shoal.

3.2.2 Hull penetration - Cargo tank opening

One of the main concerns in scenarios considering tanker collision or grounding is whether the hull is penetrated or not. Once the cargo compartment has fractured, the risk of an oil spill is impending.

The outflow of oil depends on the opening area. Potential blocking by the sea floor may reduce the effective opening. This is, however, not pursued. In the following, the evolution of the penetration area is monitored. This is done by post processing the results of the collision and grounding simulations. An examples of such a simulation is shown in Fig. 3.5. In this case the outer and inner hulls are penetrated by a rock.

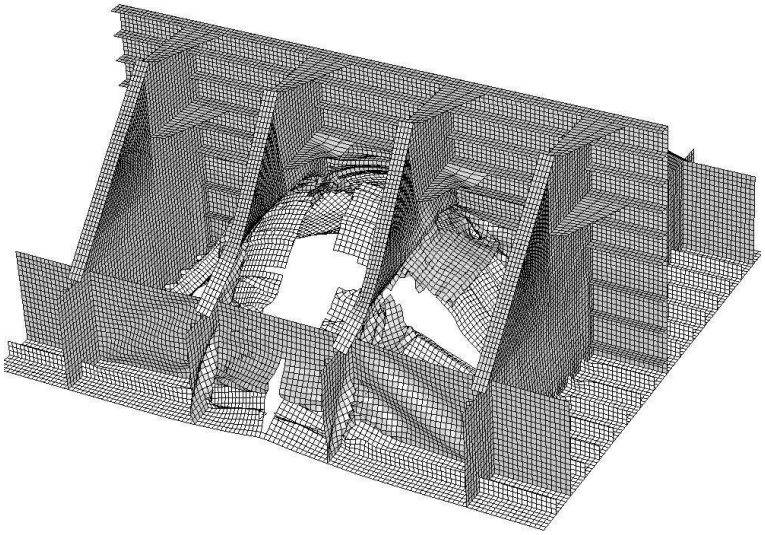

Figure 3.5: Penetration of the cargo tank; presented in [A4].

Monitoring the crack opening is done by recording the motion of the finite element nodes which convolute the crack. The node positions are read into a computer program which processes the data and produces a mesh of "triangular elements". Each of these have an area A_i, which is calculated from the vector product

$$A_i = \frac{1}{2} \mid \mathbf{a}_i \times \mathbf{a}_{i+1} \mid \tag{3.1}$$

where $\mathbf{a}_i$ and $\mathbf{a}_{i+1}$ are the vectors which describe the edges of each "triangular element", and i describes the "element" and vector number, see Fig. 3.6. Note that the area of the deleted elements are subtracted from the crack opening area. An example on the evolution of the hull opening shown for stranding on a rock is illustrated in Fig. 3.7. Both the inner and outer bottom is monitored.

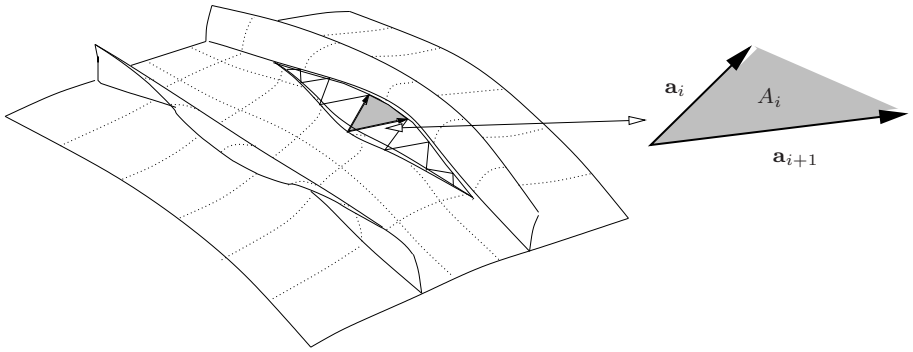

Figure 3.6: Crack opening. Crack area is calculated by triangular "elements" which are superposed.

The consequence of inner and outer hull opening is not investigated further in this thesis. The need for studies in this field is nevertheless present. An attempt on predicting the oil outflow after grounding, is performed by Tavakoli et al. (2008).

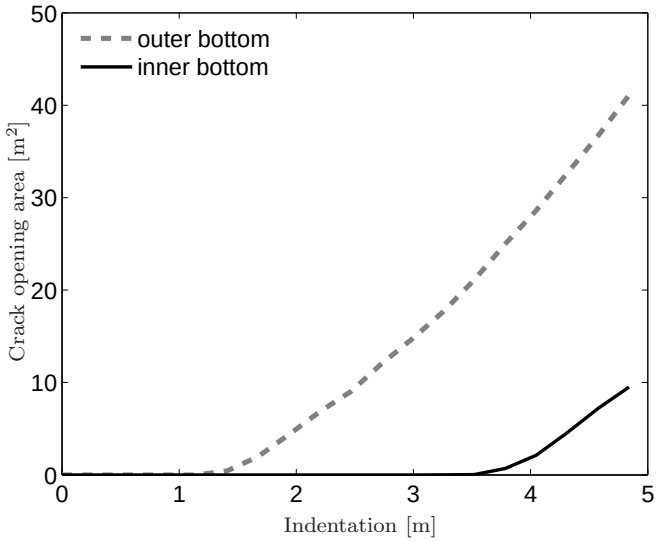

Figure 3.7: Opening of cargo tank and outer hull during grounding on a rock.

3.2.3 The sliding mechanism

Grounding with forward speed is often connected with tearing of the hull bottom and cargo tanks. This is similar to the "*Exxon Valdez*" scenario and involves impact with sharp rocks or pinnacles, which more or less cuts through the hull. Grounding on larger sea floor surfaces does not provoke this kind of damage. Instead the hull

is likely to be subjected to large contact forces which dents the ship bottom as it slides over the surface. Consequently, this is referred to as sliding damage. This is illustrated in Fig. 3.8.

The magnitude of the impact forces during a sliding event is significant. During the initial impact, grounding actions may generate dynamic bending moments and shear forces which can exceed the still water rule requirement significantly. This is dangerous with respect to the overall hull girder resistance, and has for instance been studied by Pedersen (1994) in cases of grounding on inclined slopes.

(a)

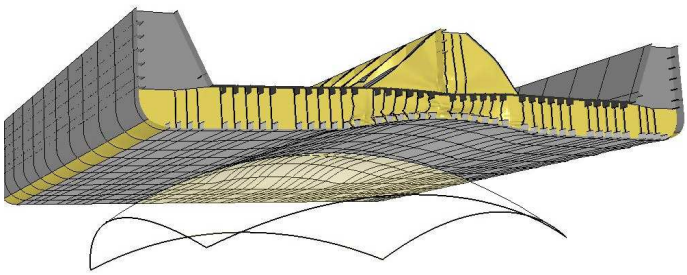

(b)

Figure 3.8: Hull damage after grounding on a shoal. Figure (a) shows the sliding damage of a ship, figure (b) illustrates simulated sliding damage.

A simplified approach to establish the sliding forces during powered grounding is presented in [A5]. This approach describes a semi-analytical method, based on assumed deformation modes during grounding on shoals. The deformation modes have been observed in parametric studies of sliding, performed in LS-DYNA. The simulations are carried out as follows: Initially the ship bottom is indented vertically

to map the resistance to indentation. This is followed by a horizontal sliding motion, see Fig. 3.9.

An interesting observations in all simulations is that once the horizontal motion is initiated, the vertical force component drops to 50% of the indentation force. The transverse and longitudinal girder webs in front of the shoal furthermore deforms similarly, both during sliding and during vertical indentation. The contact surface during vertical indentation is at the same time twice as large as the surface acting during horizontal sliding, see Fig. 3.9. Together this explains the 50% difference in vertical contact force for the two cases.

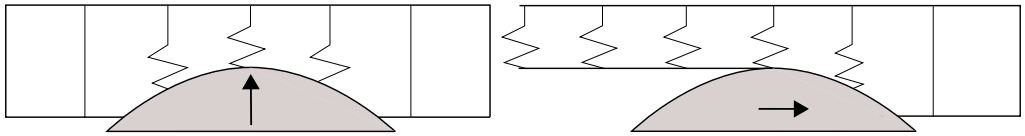

Figure 3.9: The sliding damage approach. Figure (a) illustrates vertical indentation, while figure (b) illustrates sliding process. Note that the contact surface during sliding is half the surface during vertical indentation.

It is reasonable to assume that the average contact pressure during sliding and vertical indentation is equivalent at the same indentation depth. This is substantiated by the observed correlation between contact area and contact forces during horizontal sliding and vertical indentation. In addition, the simulations reveal a similarity in the girder web crushing behavior. Consequently, if the average pressure can be assumed constant over the contact surface, it is possible to derive simplified expressions for the average sliding force components. This is based on the resistance to indentation and the shoal surface geometry, refer [A5]. For instance, sliding over a spherical shoal yields the following simplified expression for the horizontal force

$$F_x = \frac{F_R}{\pi \cos^2 \theta_0}\big(\frac{\pi}{2} - \theta_0 - \sin\theta_0 \cos\theta_0\big) + F_{fric} \tag{3.2}$$

where F_R is the vertical resistance to indentation and θ_0 describes the indentation δ in therms of a spherical angle

$$\theta_0 = \sin^{-1}\left(\frac{R-\delta}{R}\right) \tag{3.3}$$

where R is the sphere radius. F_{fric} describes the friction force, which may be expressed in terms of Coulomb's friction law. A similar derivation may also be made for the vertical force, $F_z = 1/2F_R$. The performance of the semi-analytical procedure is compared with simulated sliding forces in Fig. 3.10.

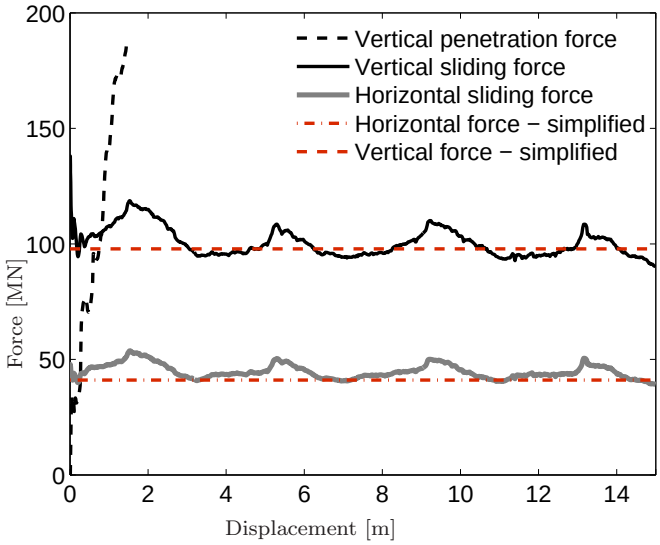

Figure 3.10: Sliding forces generated from finite element simulations and simplified considerations, Eq. (3.2).

The advantage by applying a simplified method to determine the sliding forces is that several grounding scenarios can be evaluated based on a single simulation of vertical indentation. In other words, only the resistance to indentation needs to be established, along with the surface geometry and the sliding depth. The method is applied in simplified simulations of grounding, refer section 3.4.

3.3 Global ship interaction

Until now, all analyses have focused exclusively on the internal mechanics of ship grounding. In order to fully understand grounding, the internal mechanics needs to be analyzed while interacting with the external mechanics. By doing so, the hull girder resistance can be evaluated along with the hull girder loads.

3.3.1 Hull girder response - LODIC

A grounding module has been implemented to the DSS_DC decision support tool. This grounding module is based on the ship loading calculator LODIC (LOaDIng Computer) and calculates the position of the ship based on the hydrostatic information and the internal load state, Hellan et al. (2004). The effect of grounding is represented by concentrated contact forces which correspond to certain pre-calculated stranding scenarios. These are given in [A4]. Stranding may be described by a single

point contact or a series of patch loads, if grounding takes place over a large area. At a given time the estimated grounding force is input to the load calculator. The updated mean draught, trim and roll angle in the next time increment provide the necessary information to calculate the next level of sea floor indentation and contact force. The procedure is illustrated in Fig. 3.11.

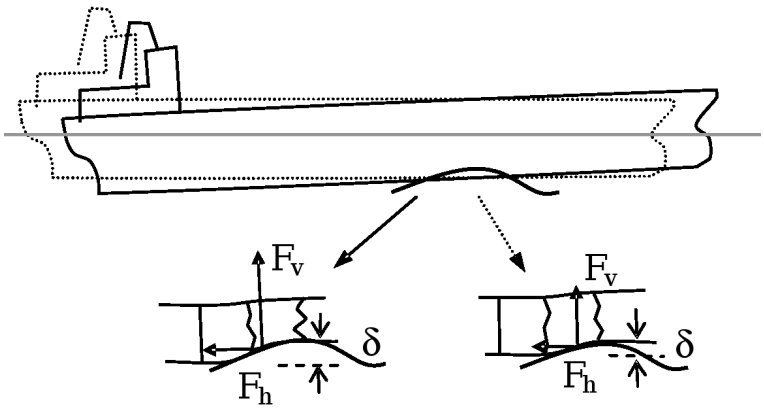

Figure 3.11: Calculation procedure - connecting local damage to global hull girder behavior.

LODIC can also assess the hull girder bending moments and shear forces. This includes the additional bending moments caused by the grounding actions. The total bending moments and shear forces are evaluated against the available hull girder capacity. Any degradation of the capacity due to bottom damage is also accounted for, see Fig. 3.12.

The rules of the ship classification societies contain requirements to the hull girder capacity in intact and damaged condition. The requirements may be used directly, but the ultimate capacity is normally somewhat higher. Roughly speaking, waves contribute by 2/3 to the total hull girder design loads. During stranding the wave loads are normally small compared to the design wave loads, so that grounding and still water loads considerably beyond still water design loads may be allowed.

3.3.2 Hull girder collapse

Large forces are involved during grounding. As shown previously, these may become significant compared to the corresponding weight of the ship. This changes the ships hydrostatic condition and may generate large hull girder bending moments. In combination with a reduced hull girder capacity, this may become critical with respect to hull girder integrity. Figure 3.13 illustrates the situation where a tanker has come to rest amidships on a shoal during a receding tide.

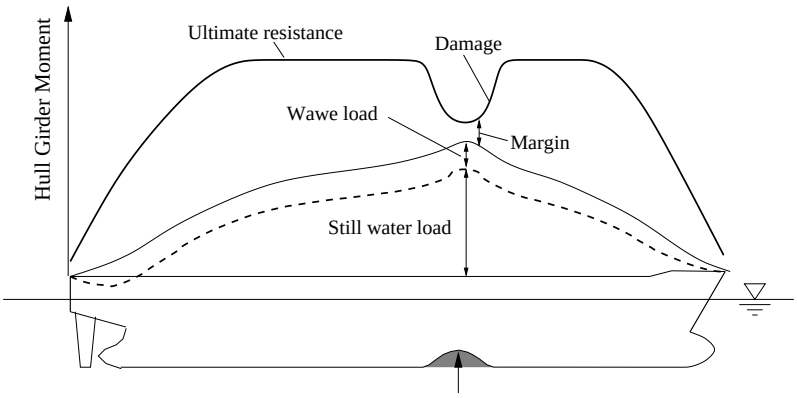

Figure 3.12: Monitoring the hull girder capacity during grounding.

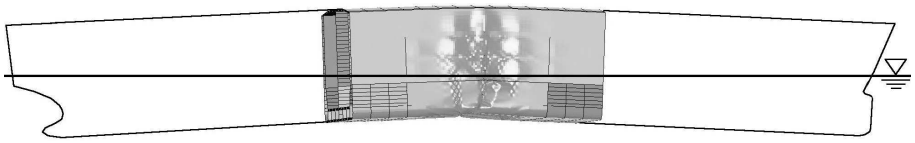

Figure 3.13: Collapse of the hull girder during stranding.

A study of the hull girder capacity during stranding is carried out in [A4]. The shuttle tanker in section 3.2 is assumed to come to rest amidships on a shoal. The stranding response of the ship is analyzed for two different still water load conditions. One corresponds to a neutral state (case 2 and 4) indicating a zero stillwater bending moment. The other scenario describes grounding at a maximum initial hogging state (case 1 and 3). The hull girder bending moment is assumed to be equal to the rule bending moment in hogging $M_0 = 4100$ MNm. Stranding is simulated for both states in LS-DYNA. The additional bending moments from changed hydrostatics is introduced by: (1) adding hogging moments from a rigid hull girder which is displaced (without pitching) out of the water by a point load (case 3 and 4); and (2) in addition taking into account the relaxation of the hogging moment when the forward and aft part of the hull girder rotate about the contact point and become immersed back into the water (case 1 and 2), see Fig. 3.13.

The force-indentation relationships for the analyses are shown in Fig. 3.14. The magnitude of the hull girder bending moments affects the global behavior of the ship significantly. The hull girder is even witnessed to collapse at some point. This occurs between 1.6 – 2 m indentation. In the case of the extreme still water hogging (case 1 and 3, $M_0 = 4100$ MNm) collapse is seen as a dramatic loss in resistance. The relaxation of the hogging moment caused by immersion of the bow and stern into the water ameliorates the situation to some degree, but only after the ship has collapsed. Further details are given in [A4].

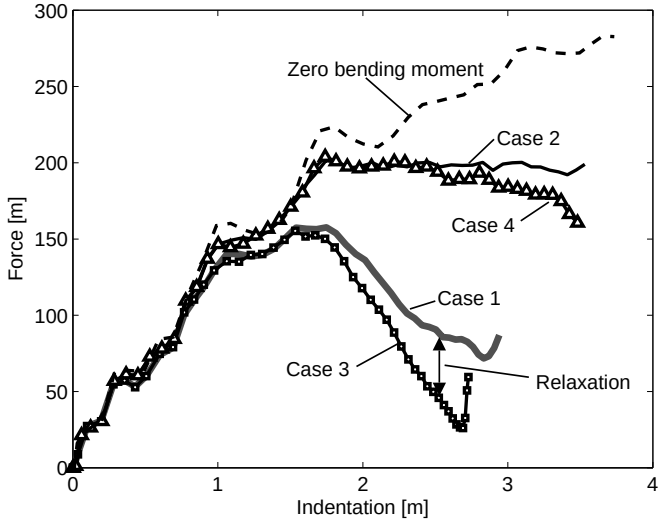

Figure 3.14: Indentation force during mid ship stranding on a shoal.

The stranding analyses show little difference in hull girder behavior before 1 m indentation. This corresponds to an indentation force around 125 MN. This indicates that a certain contact force and hull girder damage must be attained before any interaction with global bending moments should take place. It is therefore reasonable to assume that grounding on a rock can not provoke the collapse mode. As seen in section 3.2.1, the maximum attained "stranding on a rock" contact force is less than 70 MN and only local damage is observed. Grounding on a rock may therefore conveniently be simulated with a local FE model.

3.4 Dynamic grounding

Grounding of ships often occur with forward speed. This indicates a dynamic and transient ship response which complicates the analysis. Estimations of damage and hull resistance can no longer be determined by means of a prescribed indentation or sliding motion, see Fig. 3.15. Once the ship runs aground it will heave and pitch over the sea floor. Penetration is coupled to the dynamic motions of the ship, which in turn interact with the contact forces, inertia forces and hydrodynamic forces. Determining these loads is not trivial, especially since grounding by its very nature happens at shallow water depths. This complicates the hydrodynamic effects.

In [A5] work on powered grounding is briefly presented, see also Alsos and Amdahl (2007b). This is investigated by means of a simplified grounding code. The ship is assumed to slide over a shoal and is analyzed in 2 dimensions: heave, pitch and

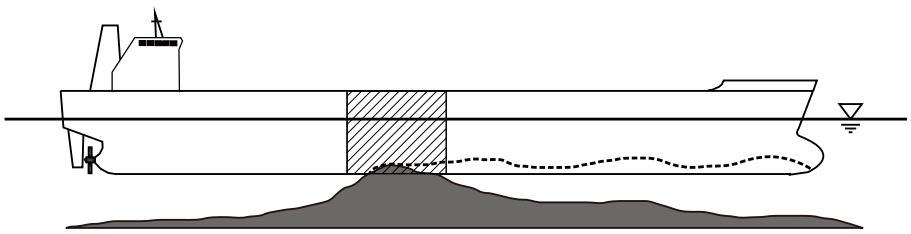

Figure 3.15: Powered grounding. The indentation of the ship bottom is controlled by dynamic effects.

surge. The computer code calculates the rigid body motions of the ship, where the grounding excitation forces are found by means of the simplified sliding force approach. Hydrodynamic loads are determined by means of constant added mass and damping terms. It is realized that this is not entirely correct. Nevertheless, in view of the uncertainties related to water depth, and the fact that grounding is very scenario dependent, this is considered satisfactory. This is furthermore justified by the fact that this is a simplified code. The ship response is found by solving the equation of motions, refer Faltinsen (1999)

$$(\mathbf{A} + \mathbf{M})\ddot{\boldsymbol{\eta}} + \mathbf{B}\dot{\boldsymbol{\eta}} + \mathbf{C}\boldsymbol{\eta} = \mathbf{F}_{ex}(\delta) \tag{3.4}$$

where $\mathbf{A}$, $\mathbf{M}$, $\mathbf{B}$ and $\mathbf{C}$ are the added mass, mass, damping and restoring matrices, respectively. The restoring term is updated during simulation. The vectors $(\ddot{\eta}, \dot{\eta}, \eta)$ denotes the acceleration, velocity, and the ship motion vectors, respectively. The final vector $\mathbf{F}_{ex}(\delta)$ describes the grounding forces in a calm waters as a function of the bottom indentation δ. The equation of motion is solved by means of the Newmark-beta integration scheme.

The tanker runs aground at 12 knots on a spherical shoal with radius 30 m. The sea floor initially "penetrates" 1.5 m into the ship hull. As the contact forces are estimated by means of the simplified sliding force approach, Eq. (3.2), it is difficult to estimate the exact bow impact force. This is because Eq. (3.2) applies the resistance to indentation relationship for the cargo area as a force input. In order to avoid an unreasonably large impact force, the sliding forces are scaled down in the initial grounding phase. This done by comparing the damaged hull volume in the impact zone with the cargo hold damage volume at the equivalent indentation. From this, a ramping function in form of a scale factor is established

$$f_{scale}(x) = \frac{V_i}{V_c} \tag{3.5}$$

where x is the contact position on the ship, and V_i and V_c, denotes the damaged volume of the impact zone and the equivalent cargo zone damage, respectively. Once contact is established in the cargo zone, f_{scale} becomes equal to unity.

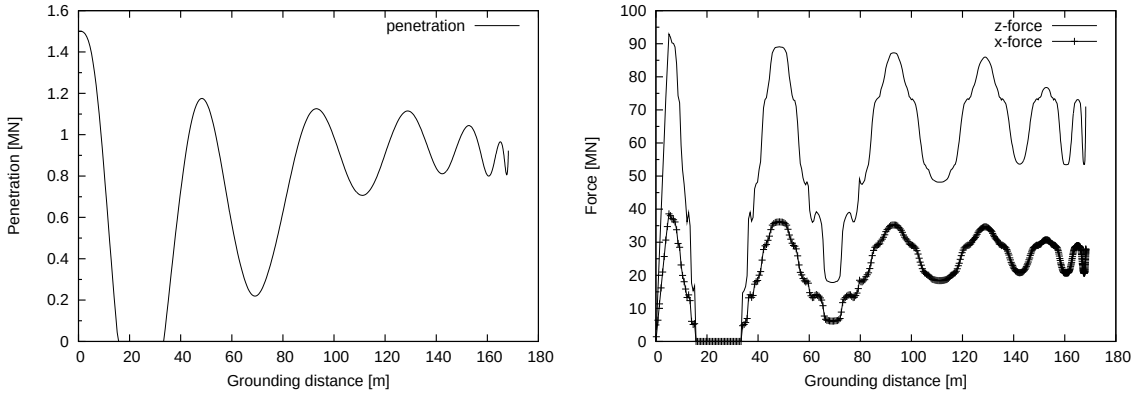

(a) (b)

Figure 3.16: Indentation (a) and contact force (b) evolution during powered grounding. Note that the force variation due to the dynamic motion is far greater than the variation caused by horizontal sliding over transverse girders, see Fig. 3.10.

The tanker response is illustrated in Fig. 3.16. The ship merely bounces up and down over the shoal. This yields oscillating contact forces and bottom damage. It is interesting to notice that the force oscillations are much larger than the force variations caused by passing transverse-girders. This becomes evident when comparing Fig. 3.10 and Fig. 3.16. Consequently, basing the contact force on an average sliding force is substantiated.

The dynamic hull girder bending moments and shear forces are plotted in Fig. 3.17, in terms of envelope curves. These describe the maximum (hogging and sagging) bending moments and shear forces recorded during the simulation. It can be observed that the dynamic hull girder loads exceed the stillwater requirements. This is especially the case for the generated shear forces, which at the impact is close to twice the stillwater rule value. Similar observations are also reported by Simonsen (1997a) and Pedersen (1994) in studies on soft grounding. Refer also Alsos and Amdahl (2007b).

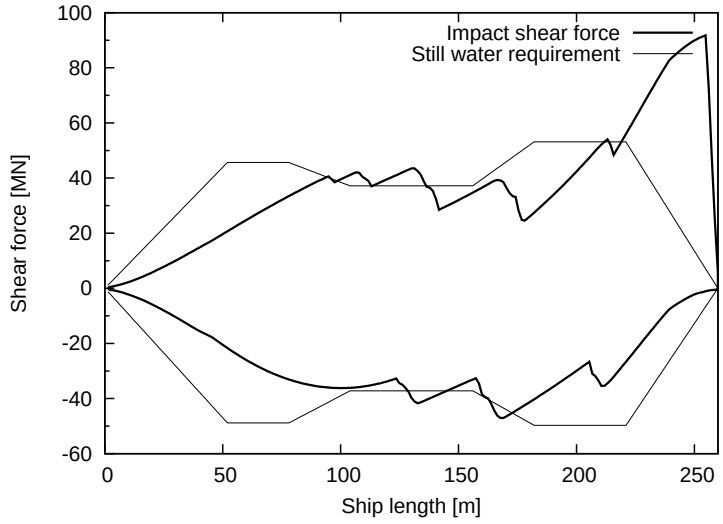

(a)

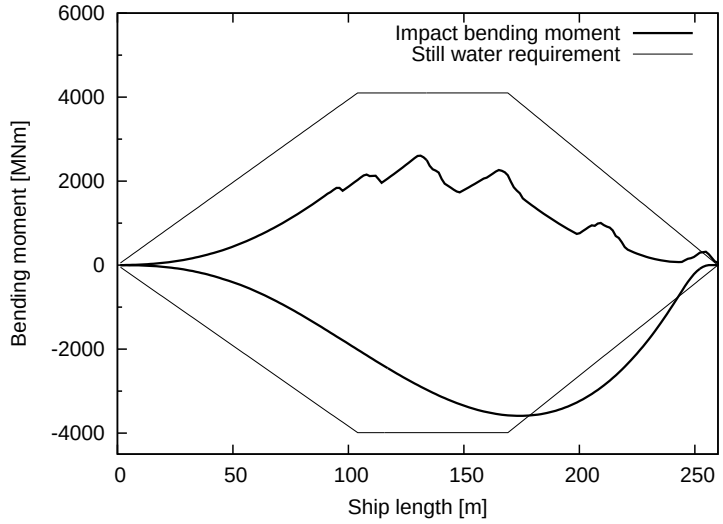

(b)

Figure 3.17: Impact shear force (a) and bending moment (b) envelope curve for the hull girder during grounding.

Chapter 4

Conclusions and recommendations for future work

The aim of the present work has been to increase the understanding and to develop/improve methods to analyze the structural behavior of ships subjected to accidental loads. This is done in cooperation with the EU sponsored DSS_DC project.

4.1 Conclusions

The present work is conducted in two separate tasks. One deals with problems related to prediction of fracture. The other deals with grounding of ships. Both tasks are closely related in the sense that the onset of fracture is a critical deformation mode during grounding. For instance, onset of fracture often implies a loss in resistance and possibly, if the cargo tank is affected; oil spill. It is therefore important to predict fracture with certain precision. Furthermore, it is equally important that this is done in a simple manner, without too much focus on calibration. Contribution to the work on fracture may be condensed in the following list:

1. The Bressan-Williams-Hill criterion is presented and verified analytically and numerically. This is a criterion which accounts for the triaxial stress state, yields good results, and is conveniently calibrated by the material stress-strain relationship..

2. The mesh sensitivity effect close to fracture is studied. A criterion to account for this effect is presented and may easily be implemented into the BWH, RTCL and any other fracture criterion.

3. The BWH and the RTCL criteria are implemented into LS-DYNA through user defined material sub routines. These sub routines automatically read

element sizes and thicknesses in order to fully automatize the failure scaling law represented by Eq. (2.14).

4. The response of stiffened panels subjected to lateral indentation is investigated. The tests have furthermore been simulated numerically using the BWH and the RTCL criterion.

5. The BWH and the RTCL criteria are applied in analyses of ship grounding in order to determine the onset of fracture.

The structural damage due to grounding is studied by means of the finite element method. The grounding response is investigated both from an internal and external mechanical point of view. In addition, attempts on coupling these aspects are made. The thesis contribution to scientific analysis of collision and grounding of ships is listed next:

1. The stranding resistance of a tanker has been investigated for various sea floor topologies. The force-indentation relations for the ships bottom are delivered, along with a Fortran communication routine to the DSS_DC grounding module (LODIC).

2. The interaction between hull girder and local damage during grounding is studied. It is shown that the global hull girder bending moment significantly affects the indentation resistance of the ship during grounding on shoals.

3. A simplified approach to determine the sliding forces during powered grounding is presented. This method is derived from the shape of the sea floor obstacle and allows simplified predictions of sliding forces. Several sliding "depths" may be calculated as long as the resistance to vertical indentation is known.

4. A two dimensional, three degree of freedom, grounding simulator has been developed. This program is applied in dynamic grounding simulations, where the hull girder bending moments and shear forces have been monitored. The grounding actions are calculated using the simplified sliding approach.

4.1.1 Work on fracture

Onset of fracture is a key factor in analyses which considers large deformations. Once initiated, a significant drop in the deformation resistance is typically observed. This behavior becomes especially important if the structure carries grounding actions in

membrane. An additional consequence of fracture is the imminent oil spill and water flooding if the hull and cargo tanks are penetrated.

Prediction of fracture is a key issue in this thesis. This is substantiated by the development of the BWH instability criterion. This criterion uniquely determines instability without need for additional calibration. The failure level is determined using Hill's analysis for local necking. This implies that onset of failure is based on the strain hardening relationship for the material, i.e. the power law exponent n.

Along with the BWH criterion, the RTCL damage criterion has been used extensively. This is an advanced criterion which also incorporates the stress triaxiality in its prediction of fracture initiation and propagation. The RTCL criterion is presented in details by Törnqvist (2003).

Fracture initiation and propagation is studied through experiments. A series of panel indentation tests is carried out on various stiffened plates. The tests show that strong stiffeners provoke early fracture in panels carrying contact forces by membrane action. The reason for this behavior is explained by that the plate deformation must take part in limited zones confined by the stiffeners. Panels with weak stiffeners, on the other hand, allow deformation to take part over a larger area. This yields a more "ductile response", which may be beneficial in sections subjected to large deformations, e.g. explosion panels and oil cargo tanks. On the other hand, it is also shown that panels with strong stiffeners have significant damaged resistance after the onset of fracture. It may seem that stiffeners guide the propagating crack within a restricted zone. This allows a load redistribution within the panel to take place. This demonstrates that initiation of fracture does not imply total loss of the panel's function. Sometimes, the post-fracture resistance may be essential for compliance with acceptance criteria in conjunction with design against accidental actions.

The panel indentation tests are successfully simulated using both the BWH and the RTCL criteria. However, as shown in the articles, predicting fracture is not trivial. At large deformations, shell elements tend to be very size sensitive, especially in zones subjected to strain consentrations. In more uniformly strained zones this effect is less apparent. This indicates that a correct handling of the mesh sensitivity effect is as important as the fracture criterion itself.

One way to reduce the mesh sensitivity effect is to make smoother transitions between structural intersections and to apply failure criteria which have less mesh sensitive properties. This may for instance be accomplished by introducing "weld elements" (elements with increased thickness) between stiffeners and plates, and is done successfully when applying the BWH criterion. However, the mesh sensitivity effect is not completely removed. Furthermore, a fine mesh is required to detect strain concentrations. In collision and grounding analyses, this approach is for the time being unrealistic. It is simply not acceptable from a computational point of view to apply elements sizes of the required size (1-4 times the element thickness).

A way to compensate for the element size sensitivity may be achieved through scaling of the critical strain level. This is done to avoid that large elements dissipate too much energy. It is, however, shown that applying failure scaling laws only yields satisfactory results in zones where large strain gradients are found. This may for instance be at crack tips, local necks, and at structural intersections. In uniformly strained areas, scaling laws are connected with poor results. It is therefore suggested that scaling laws are only applied in elements rows which are located next to structural intersections. The remaining model may have unscaled fracture properties. This is done with success (BWH and RTCL) in simulations of the panel indentation tests.

4.1.2 Grounding analyses

The double bottom damage for different stranding scenarios is investigated. The stranding scenarios consider contact on various locations as well as grounding at different sea floor topologies. An important issue in this context is the definition of a set of sea floor geometries. It is shown that the size and shape of the sea floor to a large degree determines the deformation mechanisms during grounding. The type of deformation which is provoked during grounding has therefore become the criterion for defining three types of sea floor "obstacles". These are referred to as rock, reef and shoals. For instance, stranding on rocks provoke early fracture and local damage, while stranding on a shoal introduce extensive damage to the girder-web arrangement but little fracture.

The results of the grounding calculations are implemented into the DSS_DC grounding module (LODIC), as described in section 3.3.1. This allows fast prediction of hull girder loads during grounding events. In this way, hull girder loads (bending moments and shear forces) can be compared with the damaged capacity of the ship. This information is vital for the ship master in order to take action in a grounding event, or when planning an emergency beaching of a ship.

The hull girder interaction with grounding actions and global bending moments is investigated. It is shown that when the tanker is stranded on a large shoal, the combination of contact forces, double bottom damage and formation of large bending moments eventually may provoke collapse of the hull girder. In the worst case, this is observed to occur after about 1.6 m indentation. This corresponds to a contact force equal to 150 MN and ebb in tide in the range of 3-4 m. It is concluded that stranding on a rock does not provoke the same scenario. This may be argued by the fact that generated contact forces are small and the hull damage is local. The latter scenario may therefore be simulated without including global hull girder effects.

A simplified procedure to establish the grounding forces during powered grounding is established. The grounding forces are conveniently derived from the shape

and size of the shoal contact surface, and the ships resistance to vertical indentation. This implies that the horizontal and vertical sliding forces for various indentation depths can be established based on data from a single indentation simulation. This gives a significant reduction in calculation time compared to fullscale FE simulations. The method shows promising results, even when large friction forces are applied. However, as the procedure assumes little or no fracture in the bottom plating, it should be restricted to grounding on shoals.

To exemplify the potential of the sliding force method, dynamic grounding is analyzed in two dimensions (heave, pitch and surge) using an in house ship motion calculation tool. Damage and contact forces are computed simplified by means of the simplified sliding force method. The results for a ship running aground at 12 knots on a spherical shoal, indicates a transient response where the ship merely bounces on and off the ground. This in turns creates large contact forces, hull girder shear forces and bending moments. As concluded by Pedersen (1994) and Simonsen (1997a) these distributions may easily pass the minimum bending and shear force requirements set by the classification society. A similar conclusion is also made by Alsos and Amdahl (2007b).

4.2 Recommendations for future work

The effect of the element size sensitivity at large deformations is one of the most challenging problems that still needs to be resolved. A possible procedure which involves restricting the failure scaling law to certain areas is applied with success in the simulation of the panel indentation tests. However, due to limited time to conduct further investigations, a final conclusion has not been made. Nevertheless, the procedure is promising. It is therefore recommended that it is followed up.

Further verification of the BWH and the RTCL criterion should be made, and they should be compared with results from experiments. It would also be interesting to see the criteria applied in simplified calculation methods.

All grounding simulations reported in the thesis are carried out assuming still water conditions. Nevertheless, in many cases, bad weather may be a direct cause to ship accidents, e.g. ships drifting aground after engine failure. It would be interesting to see analyses which include the weather effect in scientific studies on grounding. It is realized, though, that this is not an easy undertaking.

Most scientific analyses on ship collision and grounding focus on local hull damage and prediction of collision forces. The reason for this is obvious; to check whether the inner hull is penetrated, and to evaluate whether the ship may leak oil or flood by sea water. The next step may perhaps be studies on oil spill connected directly to the hull damage.

The powered grounding analyses have been carried out in two dimensions, only

considering heave, pitch and surge. It is recommended that this study is upgraded to a three dimensional investigation. It would also be interesting to investigate the response of a hull girder for a flexible beam and to introduce a more accurate added mass and damping terms, e.g. as presented by Simonsen (1997a).

Finally, further advance in simplified methods is attractive in view of the little computational resources which are required. This is especially the case in scenarios where large parts of the ship is damaged, e.g. during powered grounding. A significant reduction in simulation time may be achieved compared to what is possible using FEM. Although a simplified procedure is presented in this thesis, there is a need to further develop simplified methods. This may be done in therms of plastic mechanism which describe similar damage, e.g. as presented by Hong and Amdahl (2008).

Bibliography

Alsos, H. S., Amdahl, J., 2007a. On the resistance of tanker bottom structures during stranding 20, 218–237.

Alsos, H. S., Amdahl, J., 2007b. Static and dynamic analysis of a tanker during grounding. In: 10th International Symposium on Practical Design of Ships and Other Floating Structures PRADS.

Alsos, H. S., Amdahl, J., 2008a. On the resistance to penetration of stiffened plates, Part I: Experiments. Submitted to IJIE.

Alsos, H. S., Amdahl, J., 2008b. Sliding resistance of ship bottom structures subjected to grounding.

Alsos, H. S., Amdahl, J., Hopperstad, O. S., 2008a. On the resistance to penetration of stiffened plates, Part II: Numerical analysis. Submitted to IJIE.

Alsos, H. S., Hopperstad, O. S., Törnqvist, R., Amdahl, J., 2008b. Analytical and numerical analysis of local necking using a stress based instability criterion. International Journal of Solids and Structures 45, 2042–2055.

Alsos, H. S. Hopperstad, O. S., Amdahl, J., 2007c. Prediction of rupture in collision and grounding of ships using the BWH failure criterion. In: 4th International Conference on Collision and Grounding of Ships, ICCGS.

Amdahl, J., 1983. Energy absorption in ship-platform impacts. Ph.D. thesis, NTH (now Norwegian University of Science and Technology).

Amdahl, J., Kavlie, D., 1992. Experimental and numerical simulation of double hull stranding. DNV-MIT Workshop on: Mechanics of Ship Collision and Grounding.

Amdahl, J., Kavlie, D., Johansen, A., 1995. Tanker grounding resistance. In: The sixth International Symposium on Practical Design of Ships and Mobile Units, PRADS 95.

Asadi, G. V., Vaughan, H., 1990. Dynamics and structural damage of tanker ships running aground. Journal of Hazardous Materials 25, 61–73.

Atkins, A. G., 1996. Fracture in forming. Journal of Materials Processing Technology 56, 609–618.

Belytschko, T., Liu, W. K., Moran, B., 2004. Nonlinear Finite Elements for Continua and Structures. John Wiley and sons, LDT.

Bonora, N., 1997. Nonlinear cdm model for ductile failure. Engineering Fracture Mechanics 58, 11–28.

Bressan, J. D., Williams, J. A., 1983. The use of a shear instability criterion to predict local necking in sheet metal deformation. International Journal of Mechanical Sciences 25, 155–168.

Broekhuijsen, J., 2003. Ductile failure and energy absorption of y-shape test sections. Master's thesis, Delft University of Technology.

Brooking, M., Kennedy, S., September 2004. Sps design study. World and Shipbuilder, V 205, p 114-115.

Cockcroft, M. G., Latham, D. J., 1968. Ductility and the workability of metals. Journal of the Institute of Metals.

Crisfield, M. A., 1997. Non-linear Finite Element Analysis of Solids and Structures, vol 1 and 2. John Wiley and sons, LDT.

Ehlers, S., Broekhuijsen, J., Alsos, H. S., Biehl, F., Tabri, K., 2008. Simulating collision response of ship side structures; a failure criteria benchmark study. International Shipbuilding Journal, paper in press.

Faltinsen, O. M., 1999. Sea loads on ships and offshore structures. Cambridge University Press, Cambridge, United Kingdom.

Gjerstad, V., 1992. Penetration resistance of double bottom structures at grounding (in norwegian). Master's thesis, NTH (NTNU).

Goodwin, G. M., 1968. Application of strain analysis to sheet metal forming in the press shop. In: SAE paper 680093.

Gurson, A. L., 1975. Plastic flow and fracture behavior of ductile materials incorporating void nucleation. Ph.D. thesis, Brown University.

Hancock, J. W., Mackenzie, A. C., 1976. On the mechanisms of ductile failure in high-strength steels subjected to multi-axial stress-states. Journal of Mechanics and Physics of Solids 24, 147–169.

Hellan, O. ., Amdahl, A., Fiksda, G., 2004. DSS_DC SYSTEM SPECIFICATION - Intentional Grounding. Sintef Marintek report.

Hill, R., 1952. On discontinuous plastic states with special reference to localized necking in thin sheets. Journal of Mechanics and Physics of Solids 1, 19–30.

Hong, L., Amdahl, J., 2008. Plastic mechanism analysis of the grounding resistance of ship bottom longitudinal girders. To be submitted.

Hosford, W. F., Caddell, R. M., 1993. Metal forming, mechanics and metallurgy, second edition. PTR Prentice Hall.

Jetteur, P., 1986. Implicit integration algorithm for elastoplasticity in plane stress analysis. Engineering Computations 3, 251–253.

Keeler, S. P., Backhofen, W. A., 1964. Plastic instability and fracture in sheet stretched over rigid punches. ASM Trans. Quart 56, 25–48.

Kitamura, O., 2002. Fem approach to the simulation of collision and grounding damage. Marine Structures 15, 403–428.

Lehmann, E., Peschmann, J., 2001. Energy absorption by the steel structure of ships in the event of collisions. Marine Structures 15, 429–441.

Lehmann, E., Yu, X., 1998. On ductile rupture criteria for structural tear in case of ship collision and grounding. In: 7th International Symposium on Practical Design of Ships and Mobile Units PRADS98. pp. 149–156.

Lemaitre, J., 1985. A continuous damage mechanics model for ductile fracture. Journal of Engineering Materials and Technology, Transactions of the ASME 107, 83–89.

Mackenzie, A. C., Hancock, J. W., Brown, D. K., 1977. On the influence of state of stress on ductile failure initiation in high strength steels. Engineering Fracture Mechanics 9, 167–188.

Marciniak, C., Kuczynski, K., 1967. Limit strains in processes of stretch-forming sheet metal. International Journal of Mechanical Sciences 9, 609–620.

McClintock, F. A., 1968. A criterion for ductile fracture by growth of holes. Journal of Applied Mechanics, Transactions of the ASME 35, 363–371.

McCormick, M. E., Hudson, P., 2001. An analysis of the motions of grounded ships. International Journal of Offshore and Polar Engineering, 99–105.

Minorsky, V. U., 1959. An analysis of ship collisions with reference to protection of nuclear power plants. Journal of Ship Research 3, 1–4.

Naar, H., Kujala, P., Simonsen, B. C., Lundolphy, H., 2002. Comparison of the crashworthiness of various bottom and side structures. Marine Structures 15, 443–460.

Ortiz, M., Simo, J. C., 1986. An analysis of a new class of integration algorithms for elastoplastic constitutive relations. International Journal for Numerical Methods in Engineering 23, 353–366.

Paik, J. K., Amdahl, A., Barltrop, N., Donner, E. R., Gu, Y., Ito, H., Ludolphy, H., Pedersen, P. T., Rohr, U., Wang, G., 2003. ISSC Committee V.3, Collision and Grounding. International Ship and Offshore Structures Congress, San Diego, USA.

Pedersen, P. T., 1994. Ship grounding and hull-girder strength. Marine Structures 7, 1–29.

Pedersen, P. T., Zhang, S., 2000. Absorbed energy in ship collisions and grounding-revising minorsky's empirical method. Society of Naval Architects and Marine Engineers 44, 140–154.

Petersen, M. J., 1982. Dynamics of ship collisions. Ocean Engineering 9, 295–329.

Rice, J., Tracey, D., 1969. On the ductile enlargement of voids in triaxial stress fields. Journal of the mechanics and physics of solids 17, 201–217.

Rodd, J. L., Phillips, M. P., 1994. Stranding experiments on double hull tanker structures. In: The Advanced Double-Hull Technical Symposium, Gaithersburg, MD, USA.

Rodd, J. L., Sikora, J. P., 1995. Double hull grounding experiments. In: 5th. International Offshore and Polar Engineering Conference, Den Haag, The Netherlands.

Samuelides, M. S., Voudouris, G., Toulios, M., Amdahl, J., Dow, R., 2007. Simulation of the behaviour of double bottoms subjected to grounding actions. In: International Conference on Collision and Grounding of Ships.

Simo, J. C., Taylor, R. L., 1986. A return mapping algorithm for plane stress elastoplasticity. International Journal for Numerical Methods in Engineering 22, 649–670.

Simonsen, B. C., 1997a. Mechanics of ship grounding. Ph.D. thesis, DTU.

Simonsen, B. C., 1997b. Ship Grounding on Rock - I. Theory. Marine Structures 10, 519–562.

Simonsen, B. C., Hansen, P. F., 2000. Theoretical and statistical analysis of ship grounding accidents. Journal of Offshore Mechanics and Arctic Engineering, Transactions of the ASME 122, 200–207.

Simonsen, B. C., Lauridsen, L., 2000. Energy absorption and ductile failure in metal sheets under lateral indentation by a sphere. International Journal of Impact Engineering 24, 1017–1039.

Simonsen, B. C., Törnqvist, R., 2004. Experimental and numerical modelling of ductile crack propagation in large-scale shell structures. Marine Structures 17, 1–27.

Simonsen, B. C., Wierzbicki, T., 1998. Plasticity, fracture and friction in steady-state plate cutting. International Journal of Impact Engineering 21, 387–411.

Skallerud, B., Amdahl, J., 2002. Nonlinear Analyis of Offshore Structures. Research Studies Press, LDT.

Stoughton, T. B., 2000. A general forming limit criterion for sheet metal forming. International Journal of Mechanical Science 42, 1–27.

Stoughton, T. B., 2001. Stress-based forming limits in sheet metal forming. Journal of Engineering Materials and Science 123, 417–422.

Stoughton, T. B., Zhu, X., 2004. Review of theoretical models of the strain-based FLD and their relevance to the stress-based FLD. International Journal of Plasticity 20, 1463–1486.

Tautz, I., 2007. Predetermined breaking points in a ship's double hull: An innovative design concept to enhance collision safety. In: 4th International Conference on Collision and Grounding of Ships, ICCGS.

Tavakoli, M., Amdahl, J., Ashrafian, A., Leira, B., 2008. Analytical predictions of oil spill from grounded cargo tankers. In: Proceedings of the ASME 27th International Conference on Offshore Mechanics and Arctic Engineering, Estoril, Portugal.

Törnqvist, R., 2003. Design of crashworthy ship structures. Ph.D. thesis, DTU.

van de Graaf, B., Broekhuijsen, J., Vredveldt, A., van de Ven, A., 2004. Construction aspects for the schelde y-shape crashworthy hull structure. In: Preoceedings of the 3 rd. International Conference on Collision and Grounding of Ships, Izu, Japan.

Wang, G., Arita, K., Liu, D., 2000. Behavior of a double hull in a variety of stranding or collision scenarios. Marine Structures 13, 147–187.

Wang, G., Ji, C., Kujala, P., Gab Lee, S., Marino, A., Sirkar, J., Suzuki, K., Terndrup Pedersen, P., Vredeveldt, A. W., Yuriy, V., 2006. Committee V.1, Collision and Grounding. International Ship and Offshore Structures Congress, Southampton, UK.

Wang, T., Hopperstad, O. S., Lademo, O. G., Larsen, P. K., 2007. Finite element analysis of welded beam-to-coloum joints in aluminum alloy ENAW 6082 T6. Finite elements in analysis and design 44, 1–16.

Wevers, L. J., Vredeveldt, A. W., 1999. Full scale ship collision experiments. TNO-report 98-CMC-R1725, The Netherlands.

Wierzbicki, T., 1992–1999. Damage reports, joint mit-industry program on tanker safety. Tech. rep., MIT.

Wierzbicki, T., Abramowicz, W., 1983. On the Crushing Mechanics of Thin-Walled Structures. Journal of Applied Mechanics 50, 727–734.

Wierzbicki, T., Thomas, P., 1993. Closed form solution for wedge cutting force through thin metal sheets. International Journal of Mechanical Science 35, 209–229.

Wierzbicki, T., Trauth, K. A., Atkins, A. G., 1998. On Deriving Concertina Tearing. Journal of Applied Mechanics 65, 990–997.

Woisin, G., 1979. Design against collision. Shiff und Hafen 31(2), 1059–1069.

Zhang, L., Egge, E. D., Bruhns, H., 2004. Approval procedure concept for alternative arrangements. In: Proceedings of the 3th International Conference on Collision and Grounding of Ships, ICCGS.

Part II

Collection of Articles

ARTICLE I

Alsos H. S., Hopperstad O. S., Törnqvist R. and Amdahl J.

Analytical and numerical analysis of sheet metal instability using a stress based criterion

Published in:
International Journal of Solids and Structures
Vol 45, pp. 2042–2055, 2008